The Components of the CDS Bid-Ask Spreads: A Reduced-form Approach

JENNIE BAI, MAY HU, XIAOXIA YE, AND FAN YU*

May 2021

Abstract

We develop an analytical reduced-form CDS pricing model for bid and ask quotes and apply it to the term structure data of 664 single name CDS bid ask quotes covering the past nine years. We quantitatively decompose the bid-ask spreads into various components with economic implications. We find the recovery related liquidity component accounts for a large portion of the bid-ask spreads and the adverse selection components predict future changes in the CDS premiums and explain cross-sectional distribution of the CDS returns. Our analysis also reveals that the COVID-19 pandemic brings structure-breaking shocks to the CDS market making the market less competitive and efficient.

JEL Classification: G12, G13, G14, G15

Keywords: Credit default swaps, liquidity, bid-ask spreads, reduce-form model, adverse selection, loss given default, recovery, COVID-19, pandemic

*Bai (jennie.bai@georgetown.edu) is with McDonough School of Business Georgetown University and NBER, Hu (may.hu@rmit.edu.au) is with RMIT University, Ye (xiaoxia.ye@liverpool.ac.uk) is with University of Liverpool Management School, and Yu (fan.yu@claremontmckenna.edu) is with Claremont McKenna College. We thank Haoxiang Zhu for helpful comments.

1 Introduction

Understanding and estimating various components of the bid-ask spreads have long been one of the key topics in the market microstructure literature. For example, Glosten and Milgrom (1985), Stoll (1989), Affleck-Graves, Hegde, and Miller (1994), Lin, Sanger, and Booth (1995), Huang and Stoll (1997), and Menyah and Paudyal (2000), etc. The importance of this topic goes beyond the microstructure literature and contributes broadly to the asset pricing and liquidity, e.g., Amihud and Mendelson (1986, 1989). The bid-ask spread is not only important in the equity market, it is also key to understanding the CDS market. With the fast growth of the CDS market (see, e.g., Longstaff, Mithal, and Neis, 2005; Oehmke and Zawadowski, 2017), the liquidity in the CDS market has also attracted increasing attentions in the literature, e.g., Bongaerts, De Jong, and Driessen (2011), Loon and Zhong (2016), Tang and Yan (2017), and Collin-Dufresne, Junge, and Trolle (2020). However, to the best of our knowledge, none of these studies have explicitly quantified the components of the bid-ask spreads in the CDS market. As one of the key aspects of the liquidity, quantifying these components is of crucial importance in understanding the liquidity and structure of the CDS market.

Unlike conventional securities such as stocks and corporate bonds, each CDS contract has two legs: the protection leg and the premium leg. Dealers in the CDS market have different considerations for the two legs when quoting bid and ask CDS premiums. This unique security design renders a natural identification scheme for modeling various components in the CDS bid and ask quote spreads. In this paper, capitalizing on this identification scheme and the growing availability of the CDS bid-ask spreads data in recent years, we systematically study the components of the CDS bid-ask quotes via the lens of a reduced-form model novelly designed to decompose the CDS bid-ask spreads.

Specifically, we identify five components in the CDS bid-ask spreads: *adverse selection*, *monopolist profits*, *inventory costs*, *loss given default* (LGD), and *counterparty risk*. The first three components have been commonly studied in the equity market bid-ask literature (see the references above). The last two ones are unique in the CDS market. We use a constant default

intensity version of the reduced-form CDS pricing model of Longstaff, Mithal, and Neis (2005) as the benchmark model. The fact that the CDS premiums are priced from equalizing two legs allows us to model the different components through the two legs in the bid and ask CDS premiums. For example, the buy (sell) side adverse selection and monopolist profits (counterparty risk) only appear in the ask (bid) quote, while the credit default intensity enters into both bid and ask quotes. Building on this fact, we extend the benchmark model and link the five different components to the bid and ask quotes analytically. By construction, our model also admits of a flexible term structure for the bid/ask quotes.

We calibrate the model to 664 firms' Single-name CDS bid ask quotes on various maturities over a sample of nine years (from November 2011 to November 2020). The calibrated model quantifies the observed term structure of bid-ask spreads into the term structure of the five components. We find that the recovery-related liquidity component accounts for a big portion of the bid-ask spreads: about 80% for five-year CDS quotes and even higher for longer maturities, but down to about 50% of the bid-ask spreads at shorter maturities. This monotonic pattern is understandable as the recovery-related liquidity increases with the horizon at a decreasing rate. The next two largest components are the adverse selection from the sell and buy sides. The sell side adverse selection is more sizeable on shorter maturities while the buy side weights more on longer maturities. This asymmetric maturity effect between the sell side and buy side reflects informed traders' rational behaviour.[1] However, the portion of the sell side at the short end (over 40% on average) is significantly larger in that of the buy side at the long end (about 6% on average). The fourth component in size is the monopolist profits, which counts for over 5% of the bid-ask spreads on average and is concentrated in mid maturities only. The remaining other components are relatively small in size.

The empirical results yield a number of interesting and novel observations: i) the adverse selection components have a clear U-shape term structure with the sell side much higher than

[1] A CDS curve is normally low and upward sloping, but occasionally when risk rises, it becomes high and downward sloping. So informed buyers will use long-term contracts to avoid dealing with spikes in short-term CDS spreads when rolling them over. Informed sellers will use short-term contracts because these will fall the most when risk level drops.

the buy side, indicating the dealers are concerned more with the adverse selection from the sell side than from the buy side on maturities other than five-year; ii) the monopolist profits are concentrated on maturities near five-year where the majority of CDS contracts are traded on; iii) the counterparty risk accounts for little of the bid-ask spreads for years before the COVID-19 pandemic. This observation is consistent with Arora, Gandhi, and Longstaff (2012) and the fact that the CDS market participants require collateralization of swap liabilities by counterparties. However, when the pandemic happens the counterparty risk becomes a sizeable component in the bid-ask spreads due to the acute uncertainty; iv) the recovery-related liquidity has significant weights in the bid-ask spread and the longer maturity the higher weights, indicating the liquidity in the CDS market has a close connection with the liquidity in the corporate bond market; and v) during normal times when mass clustered defaults are rare, the inventory costs for hedging purposes are higher when dealers are receiving premiums than paying premiums due to the cash flow management; while during extraordinary times, the reverse applies due to dealers' heightened risk-averse to defaults when facing radical uncertainty.

One of the original purposes of decomposing the bid-ask spreads is to identify the adverse selection component. As articulated in Stoll (1989), the adverse information cost due to adverse selection from informed traders has predictive power on the expected equilibrium price. We test this prediction using the identified adverse selection components and five-year CDS mid quotes. More concretely, we first regress the daily changes of the five-year CDS spreads to the lagged changes of the adverse selection while controlling for other components. The statistical significance of the regression coefficients confirms that when the adverse selection from the buy (sell) side increases, the dealers are likely to adjust their ask (bid) price upwards (downwards) the next day. Ceteris paribus, the next day's mid price will increase (decrease). Second, we use the portfolio sorting analysis commonly used in the asset pricing literature to study the adverse selection components' explanatory power on the cross-sectional CDS returns. The results show that the high-minus-low portfolio formed from sorting the adverse selection components generates a monthly return of 1.2% (t-statistic = 2.3) while the portfolio formed based on the

raw bid-ask spreads generates an significant monthly return of -0.5% (t-statistic = -0.5). The results confirm that the model implied adverse selection components carry important information useful for asset pricing in the CDS market, which is otherwise unavailable in the CDS bid-ask spreads per se.

As our data cover the outset of the COVID-19 pandemic, our study also sheds light on the market liquidity dynamics and the dealers' reactions during the pandemic. We find that at the beginning of the pandemic, both the level and cross-sectional dispersion of the bid-ask spreads increase significantly. Our model disaggregates these shocks into changes in the different components: the buy side adverse selection component drops while the sell side adverse selection shoots up. Meanwhile, the monopolist profits and counterparty risk both increase. Note that the counterparty risk component has historically been low. Although the absolute recovery-related liquidity component deepens, its relative term actually shrinks, indicating the CDS market specific uncertainty crowds out the corporate bond market liquidity concerns in the CDS bid-ask spreads during the pandemic. Overall, the COVID-19 induced uncertainty has made the CDS market less competitive and brought more informational frictions. From studying the inventory costs during the pandemic, we also find that the CDS dealers are highly risk-averse when facing radical uncertainty. Haddad, Moreira, and Muir (2020) and Chen et al. (2021) find that COVID-19 crisis has created similar disruptions to dealers in other fixed income markets, e.g., corporate bond market and market back security (MBS) market.

This paper contributes to three areas in the literature. Firstly, our study relates to the liquidity of the CDS market. Bongaerts, De Jong, and Driessen (2011) develop an an equilibrium asset pricing model featuring liquidity risk and derivative pricing. They apply the model to the CDS market and find that the credit protection sellers earn a liquidity premium. Our empirical results support their findings. Loon and Zhong (2016) study how Dodd-Frank reforms effect the transaction costs and liquidity in the CDS market and find these reforms lower trading costs, price impact, and price dispersion. Tang and Yan (2017) find that the CDS premiums are not only driven by fundamental credit risk factors, but also by market liquidity.

Collin-Dufresne, Junge, and Trolle (2020) study the liquidity and market structure of the *index* CDS market after the implementation of the Dodd-Frank Act. They find that transaction costs are higher for dealer-to-client than interdealer trades and the market structure is largely explained by the different characteristics of client trades, which are relatively infrequent, large, and differentially informed. However, none of these studies have attempted to look into the components of the single name CDS bid-ask spreads. To the best of our knowledge, we are the first to provide a novel analytical tool that quantifies the different components of the bid-ask spreads and empirical results that help understand the liquidity of the CDS market from brand-new angles.

Second, our paper also contributes the traditional literature on the components of the bid-ask spreads. For example, Glosten and Milgrom (1985), Stoll (1989), Affleck-Graves, Hegde, and Miller (1994), Lin, Sanger, and Booth (1995), Huang and Stoll (1997), and Menyah and Paudyal (2000), etc. The uniqueness and novelty of our study lie in the fact we adopt a reduced-form credit derivative pricing model, which differs from the approach used in the traditional market microstructure literature, and study the components of the bid-ask spreads in the CDS market, which has been largely overlooked in the traditional literature that has mostly focused on the equity market.

Third, the novel CDS pricing model developed in our paper contributes to the literature on the reduced-form modeling for the credit derivative pricing, see, e.g., Duffie (1999), Duffie, Pedersen, and Singleton (2003), and Longstaff, Mithal, and Neis (2005). The key novel feature we bring to the reduced-form modeling is the analytical solutions connecting the different components to the bid and ask quotes. Thanks to the analytical nature of the framework, our model is appealing to practical applications. For example, the model can be easily and quickly calibrated to large scale of CDS bid-ask spreads term structure data even on a daily basis to exact information about the different components for trading and monitoring purposes.

The rest of this paper is organized as follows. In Section 2, we develop the reduced-form CDS pricing framework for the bid and ask quotes. Section 3 discusses the data used to calibrate

the model. Section 4 presents a case study on the historical dynamics of T-mobile's CDS bid-ask spreads. We present and discuss empirical results in Section 5. Section 6 concludes. The appendices contain proofs and a specification analysis.

2 A reduced-form model for the CDS quotes

To concentrate on the default and liquidity related factors, i.e., default intensity, loss given default (LGD), adverse selection, monopolist power, inventory costs, and counterparty risk, we abstract the modeling from the interaction with the interest rate by setting it to zero. Also, to make the modelling more intuitive, we assume deterministic factors. In Appendix B, using a more dynamic and sophistic modeling framework, we show that the constant default intensity assumption has negligible misspecification issue in estimation when frequent recalibration is applied.

2.1 Benchmark quote

There are no liquidity issues or market friction at all in the benchmark quote model. The CDS premium is set to be a function of the loss given default and the default intensity. Specifically, following Longstaff, Mithal, and Neis (2005), we assume that the premium is paid continuously. For time to maturity Δt, the premium leg $Q_{\Delta t}$ and protection leg $P_{\Delta t}$ are given as:

$$Q_{\Delta t} = s_{\Delta t} \int_0^{\Delta t} e^{-\lambda \tau} d\tau,$$
$$P_{\Delta t} = w\lambda \int_0^{\Delta t} e^{-\lambda \tau} d\tau.$$

The CDS spread is the $s_{\Delta t}$ equalising $Q_{\Delta t}$ and $P_{\Delta t}$, i.e.,

$$s_{\Delta t} = \frac{w\lambda \int_0^{\Delta t} e^{-\tau\lambda} d\tau}{\int_0^{\Delta t} e^{-\tau\lambda} d\tau} = w\lambda.$$

where w is the LGD and λ is the default intensity. Apparently in this most simplified form, the term structure of CDS premium is flat and fixed just at the product of LGD and default intensity.

2.2 Adding liquidity premium to LGD

Realised LGD is associated with uncertainty and depends on the liquidity and efficiency of the defaulted corporate bond markets (both the CDS auctions and the secondary market, see Du and Zhu, 2017 for more details). We capture this by using a liquidity convenience yield η (Longstaff, Mithal, and Neis, 2005) to discount recovery given default $(1 - w)$. That is, the protection leg is now given as

$$P_{\Delta t} = \lambda \int_0^{\Delta t} \left[1 - (1 - w) e^{-\tau\eta}\right] e^{-\tau\lambda} d\tau,$$

and CDS premium is:

$$s_{\Delta t} = \frac{\lambda \int_0^{\Delta t} \left[1 - (1 - w) e^{-\tau\eta}\right] e^{-\tau\lambda} d\tau}{\int_0^{\Delta t} e^{-\tau\lambda} d\tau} = \lambda \left[1 - \frac{g(\lambda + \eta, \Delta t)}{g(\lambda, \Delta t)} (1 - w)\right], \tag{1}$$

where $g(x, \tau) = \frac{1 - e^{-x\tau}}{x}$. We can see that even both η and λ are constant, when LGD depends on liquidity of the corporate bond market, we can have a non-trivial term structure of CDS premium.

2.3 Bid-ask quote modeling

From the classic literature on bid-ask spreads, such as Glosten (1989), Glosten and Harris (1988), Glosten and Milgrom (1985), Huang and Stoll (1997), and Stoll (1989) etc., the key components of bid-ask spreads identified previously are adverse selection, monopolist profits, and inventory costs. Due to the nature of the CDS market, counterparty risk (Jarrow and Yu, 2001), the risk that the counterparty could not make the promised payment, is an important component of CDS bid-ask spreads but of little relevance in the classic bid-ask spreads literature focusing on

the equity market. Similarly, the recovery-related liquidity is unique to the CDS market and has asymmetric effects on bid and ask quotes. Therefore, the recovery-related liquidity is also an important component in the CDS bid-ask spreads that has been overlooked in the previous bid-ask spreads literature.

Adverse selection This is an inevitable consequence of asymmetric information, which is especially significant in the CDS market where insider trading has been concerning (see, e.g., Acharya and Johnson, 2007).

Monopolist profits This happens when a market has a high level of concentration. The CDS market has exactly this feature (see, e.g., Arce, Gonzalez Pueyo, and Sanjuán, 2010; Deventer, 2012). Jarrow et al. (2018) also point out that the high level of concentration could lead to market manipulations and persistent mispricing.

Inventory costs These are costs to cover losses due to unhedged risk exposure or high hedging costs. Most of the CDS market players are sophisticated institutional investors (e.g., investment banks, commercial banks, insurance companies, and hedge funds) whose investment portfolios are believed to be well-diversified. We expect the inventory costs to be a relatively small component in absolute terms comparing to the adverse selection cost.

LGD and counterparty risk These two are special features of the CDS market that have not been linked with bid-ask spreads in previous studies.

We now show that all these factors can be coherently modelled within our simple framework thanks to the separation of the premium leg Q and the protection leg P.

2.3.1 Ask quote

For an ask quote, the quoting dealer is a potential CDS seller. From a seller's perspective, the adverse selection is factored in to the quote through adjusting the default intensity upwards, i.e., $\lambda_A = \lambda + l_A$, where $l_A > 0$, while the counterparty risk is understandably less of a concern.

Regarding the monopolist profits, we model them through another convenience yield $\gamma_A > 0$ which discounts the counterparty's premium payment in $Q_{A,\Delta t}$. Putting together, we have

$$
\begin{aligned}
Q_{A,\Delta t} &= s_{A,\Delta t} \int_0^{\Delta t} e^{-\tau(\lambda_A+\gamma_A)} d\tau, \\
P_{A,\Delta t} &= \lambda_A \int_0^{\Delta t} \left[1-(1-w)\, e^{-\tau\eta}\right] e^{-\tau\lambda_A} d\tau,
\end{aligned}
$$

and the CDS premium ask quote is

$$
s_{A,\Delta t} = \lambda_A \frac{g\left(\lambda_A, \Delta t\right)}{g\left(\lambda_A+\gamma_A, \Delta t\right)} \left[1 - \frac{g\left(\lambda_A+\eta, \Delta t\right)}{g\left(\lambda_A, \Delta t\right)} (1-w)\right]. \tag{2}
$$

2.3.2 Bid quote

For a bid quote, the quoting dealer is a potential CDS buyer. From a buyer's perspective, the adverse selection is factored in to the quote through adjusting the default intensity downwards, i.e., $\lambda_B = \lambda - l_B$, where $0 < l_B < \lambda$. Unlike a seller, from a buyer's perspective the counterparty risk is a crucial consideration as the realization of the protection payment in case of default depends on the counterparty's solvency. The counterparty risk $\gamma_B > 0$ is factored into the quote through discounting the LGD. Therefore, we have

$$
\begin{aligned}
Q_{B,\Delta t} &= s_{B,\Delta t} \int_0^{\Delta t} e^{-\tau\lambda_B} d\tau, \\
P_{B,\Delta t} &= \lambda_B \int_0^{\Delta t} \left[1-(1-w)\, e^{-\tau\eta}\right] e^{-\tau(\lambda_B+\gamma_B)} d\tau,
\end{aligned}
$$

and the CDS premium bid quote is

$$
s_{B,\Delta t} = \lambda_B \frac{g\left(\lambda_B+\gamma_B, \Delta t\right)}{g\left(\lambda_B, \Delta t\right)} \left[1 - \frac{g\left(\lambda_B+\gamma_B+\eta, \Delta t\right)}{g\left(\lambda_B+\gamma_B, \Delta t\right)} (1-w)\right]. \tag{3}
$$

2.3.3 General properties of the model

Intuitively, by construction the bid-ask spread $BA_{\Delta t} = s_{A,\Delta t} - s_{B,\Delta t}$ of CDS premium is positive and increases with the adverse selection l_A and l_B, the monopolist profits γ_A, and counterparty risk γ_B. Clearly, $BA_{\Delta t}$ should also be affected by the LGD factors w and η. Under some modest conditions, $BA_{\Delta t}$ increases with w and η as well. These intuitions are formally confirmed in the following proposition and proved in Appendix A.

Proposition 1 *Given positive λ, l_A, η, γ_A, γ_B, and $0 < w \leq 1$ and $0 < l_B < \lambda$, for any $\Delta t > 0$ the following are true:*

1. $\frac{\partial s_{\Delta t}}{\partial \lambda} > w$, $\frac{\partial s_{A,\Delta t}}{\partial \lambda_A} > w$, and $\frac{\partial s_{B,\Delta t}}{\partial \lambda_B} > 0$;
2. $BA_{\Delta t} = s_{A,\Delta t} - s_{B,\Delta t}$ is positive;
3. $\frac{\partial BA_{\Delta t}}{\partial \gamma_A} > 0$, $\frac{\partial BA_{\Delta t}}{\partial \gamma_B} > 0$, $\frac{\partial BA_{\Delta t}}{\partial l_A} > 0$, and $\frac{\partial BA_{\Delta t}}{\partial l_B} > 0$;
4. $\frac{\partial BA_{\Delta t}}{\partial w} > 0$ if $\gamma_A > \eta$, and $\frac{\partial BA_{\Delta t}}{\partial \eta} > 0$ if $l_A + l_B > \gamma_B$.

It is worth noting that, in a rigorous sense, both l_A and l_B should be understood as the net effect of the adverse selection and the inventory cost. Specifically, when the buy (sell) side adverse selection increases, the dealer raises (lowers) the ask (bid) quote by adjusting λ to $\lambda_A^0 = \lambda + l_A^0$ ($\lambda_B^0 = \lambda - l_B^0$), but at the same time the dealer could also raise (lower) the bid (ask) quote to increase the chance of opposite transactions for hedging purposes, e.g., adjusting λ_B^0 to $\lambda_B = \lambda_B^0 + \alpha l_A^0$ (λ_A^0 to $\lambda_A = \lambda_A^0 - \beta l_B^0$) where $\alpha \geq 0$ ($\beta \geq 0$). Therefore, we have $l_A = l_A^0 - \beta l_B^0$ and $l_B = l_B^0 - \alpha l_A^0$. Introducing α and β adds little complexity to the model but reduces the parameter identification at the calibration stage. So we only keep l_A and l_B in the calibration, and in the empirical section, we quantify α, β, l_A^0 and l_B^0 using linear regressions based on the calibrated l_A and l_B.

2.4 Term structure of bid-ask spreads

There is a term structure pattern in bid-ask spreads: a U-shape term structure with five-year being the lowest one and six-month and 10-year (or longer) being the higher ones. An example of this term structure is presented in Figure 1.

[*Insert Figure 1 about here*]

To capture any heterogeneity in the factors across maturities, we allow a flexible term structure for l_A, l_B, γ_A and γ_B, while we expect λ, η, and w to have only a flat term structure as these are not contract-specific. More concretely, we allow three free parameters in the term structure function for $l_A(\Delta t)$, $l_B(\Delta t)$, $\gamma_A(\Delta t)$ and $\gamma_B(\Delta t)$ to pin down three values at six-month, five-year, and 10-year then interpolate the term structure curve using spline function to fill the values on any points in between six months and 10 years. Since we only have maximal 14 values (seven CDS premiums and seven bid-ask spreads) at each point in time, to avoid under-identification issue, we set $w = 1 - e^{-\lambda}$. This simplification is consistent with the fact that the historical LGD statistically increases with the default risk (Altman et al., 2005; Meng et al., 2010).

3 Data

We use Markit's CDS Liquidity Metrics data and focus on US Senior Unsecured Debt single names. The data consist of daily bid-ask spreads and mid-quotes of the conventional CDS premium, covering November 2011 to November 2020. There are eight maturities: six-month, one- to five-year, seven-year and 10-year. Markit provides Liquidity Scores[2] as a measure for the liquidity quality of the quotes and bid-ask spreads. To ensure the most reliable and executable quotes, we restrict ourselves to data with the Liquidity Scores no higher than two. In the end, we have 664 unique firm tickers in our sample.

[2]It is a scale between one and five with one being the most liquid. See IHS Markit CDS Liquidity user guide for more details.

[*Insert Table 1 about here*]

We present the summary descriptives of one-, five-, and 10-year data in Table 1. The mid quotes increase monotonically with maturities, while the bid-ask spreads exhibit a clear U-shape term structure. The time series of cross-sectional average of the data are plotted in Figure 2. We also plot CDS notional related time series over the sample period in Figure 3. One observation worth noticing is that the net notional outstanding continues to decline over the years. A similar pattern has been documented in Oehmke and Zawadowski (2017, the dotted line in Figure 2) in their sample from 2009 to 2013. Our data confirm that the downward trend extends beyond 2013 and continues till recent years. As pointed out in Aldasoro and Ehlers (2018), the decline in inter-dealer positions has coincided with the rise of central counterparties (CCPs), which is likely a key driving force of the decline. Our sample starts from the peak of the European sovereign debt crisis and ends at the first wave of the Covid-19 pandemic. The time series of the average CDS mid quotes (the mid panel in Figure 2) sees two big spikes corresponding to these two crises.

[*Insert Figures 2 and 3 about here*]

From the left and middle panels in Figure 2, we also observe that at the outset of the COVID-19 pandemic, both the CDS premiums and bid-ask spreads spike significantly. They then quickly drop to lower than the pre-pandemic level. In absolute terms, the short term bid-ask spreads spike the most (the left panel in Figure 2). In relative terms (comparing to the CDS mid-quote), the spike is only observed in the long term relative bid-ask spreads, the short term relative bid-ask spreads drop at the outset of the pandemic. This means although the short term CDS premiums spike more dramatically than the short term bid-ask spreads, while the long term bid-ask spreads spike more dramatically than the CDS premiums.

From the middle panel in Figure 3, we find the net notional outstanding of CDS trading drops nearly half during the outset of the pandemic. It comes back to the pre-pandemic level (even slightly higher), but drops again towards the end of our sample (November 2020). This shows the Covid 19 epidemic "Waves" induce high volatility into the CDS trading activities.

4 A case study: T Mobile USA Inc

In this section, we present a case study using T-Mobile USA Inc's CDS premiums and quoted bid-ask spreads panel data. The overview of the panel data is shown in Figure 4. We first calibrate the model to the time-series average of CDS premiums and bid-ask spreads. The calibration is done by minimizing the mean squared deviation of the difference between model-implied bid and ask quotes and observed bid and ask quotes on various maturities. Standard numerical optimization algorithms can be used for the calibration, e.g., simplex search method and Quasi-Newton method. The model can fit the data well: it captures both CDS premium term structure and bid-ask spreads term structure. The model results v.s. data are presented in Figure 5. Then, we calibrate the model to the term structures of the CDS premiums and bid-ask spreads at each point in time and infer time series of the different components. Thanks to the analytical solutions of the model, the numerical procedure used in the calibrations converges quickly, making large scale computation feasible.

[*Insert Figures 4 and 5 about here*]

4.1 Components of the bid-ask spread

Given the calibrated model, we are able to decompose the bid-ask spread into different components discussed in the previous section. Namely, we look at the adverse selection from both sell side and buy side (setting l_B and l_A to zero), the recovery-related liquidity (setting η to zero), the monopolist profits (setting γ_A to zero), and the counterparty risk from sell side (setting γ_B to zero). The decomposition is presented in Figure 6. There are a few novel insights: a) the adverse selection components clearly have a U-shape term structure. The dealers seem to be concerned more with the adverse selection from the sell side than from the buy side when the contracts under consideration are on the nonstandard maturities. In other words, the dealers seem to believe that buyers on the nonstandard maturities are more likely to have a genuine need for hedging but sellers on the nonstandard maturities could use their

informational advantages to earn premiums. To a certain extent, this insight is in line with Bongaerts, De Jong, and Driessen (2011)'s finding on liquidity premium earned by credit protection sellers; b) the monopolist profits concentrate on the middle range maturities where the majority of contracts are traded on; c) the counterparty risk accounts for little of the bid-ask spreads. This observation is consistent with Arora, Gandhi, and Longstaff (2012) and the fact that the CDS market participants require collateralization of swap liabilities by counterparties; d) the recovery-related liquidity has significant weights in the bid-ask spread and the longer maturity the higher weights. Since the recovery-related liquidity is related to the corporate bond market liquidity, our results show that the liquidity in the CDS market has a close connection with the liquidity in the corporate bond market, especially the defaulted corporate bond markets, i.e., the CDS auction market and corporate bond secondary market.

[*Insert Figure 6 about here*]

We also look at the across-maturity averages of the different components over time. The time series are presented in Figure 7. From 2013 to 2020, the adverse selection from sell side and the recovery-related liquidity have been the main driving forces behind the bid-ask spreads dynamics, especially after 2015, while the counterparty risk component has been even more negligible in recent years. Although smaller in magnitude than the adverse selection from sell side and the recovery-related liquidity, the adverse selection from buy side and the monopolist profits are significant and relatively steady over the years.

[*Insert Figure 7 about here*]

4.2 Liquidity impounded in the CDS premium

Our model also allows us to shed light on how the components in bid-ask spreads are impounded in the CDS premiums. A decomposition similar to Figure 6 can be done for the CDS mid-quote $\frac{s_{A,\Delta t}+s_{B,\Delta t}}{2}$. Since trades normally happen between bid and ask quotes, the CDS mid-quote can be regarded as a proxy for traded CDS premiums. This CDS mid-quote

decomposition is presented in Figure 8. As expected, the recovery-related liquidity and default risk are the primary components in the CDS mid-quote. Interestingly, we can see the adverse selection from sell side has negative effects on the CDS premiums at the short and long ends of the maturities. This is because a positive l_B set by the dealers to discourage insider selling at the short and long ends of the maturities has made the CDS premium lower than otherwise. The monopolist profits show up positively in the CDS mid-quote at the middle range maturities, which is consistent with Bongaerts, De Jong, and Driessen (2011)'s finding on liquidity premium earned by credit protection sellers. We also show the time series of the across-maturity averages of the decomposition in Figure 9. We find the negative effect of the adverse selection from sell side on the CDS premium has become more noticeable after 2015.

[*Insert Figures 8 and 9 about here*]

5 Empirical results

5.1 General observations

The overall distributions (over time and cross firms) of the bid-ask spreads components at different maturities is presented in Figure 10. The main take away message from these distributions is consistent with the observations from Section 4. This consistency warrants the robustness and generality of our model.

[*Insert Figure 10 about here*]

To see how these components change over time, we plot the cross-sectional distributions of the five-year CDS bid-ask spreads components at each point in time in Figure 11. Before the outbreak of the COVID-19 pandemic, three observations are worth noting. First, the counterparty risk component has been small for years after 2013 before the outbreak of the pandemic (the two γ_B plots in Figure 11). This is consistent with Aldasoro and Ehlers (2018)

who find that "CCPs are likely to have been a key driver behind the reduction in inter-dealer positions and notional amounts outstanding in recent years," and "increased clearing via CCPs has helped to reduce counterparty risks", a notion that has been theoretically and empirically verified, see, e.g., Duffie and Zhu (2011)[3] and Loon and Zhong (2014).

Second, the monopolist profits has been decreasing for years before the outbreak of the pandemic. The downward trend is obvious from 2012 to 2019. This is a clear sign of market competition improvement over the years. This is likely thanks to the Dodd-Frank act enacted on July 21, 2010 (Loon and Zhong, 2016).

Third, during the European sovereign debit crisis (2011 to 2013) at the start of our sample (Panel (b) of Figure 11), we see relatively low (high) adverse selection from buy (sell) side and relatively high monopolist profits. This is a typical observation during a crisis period as we also see a similar pattern in the COVID-19 pandemic at the end of our sample. We explain the intuition in details in the next subsection.

[*Insert Figure 11 about here*]

5.2 Impact of the COVID-19 pandemic

March 2020, the COVID-19 pandemic burst out globally. The outbreak of the pandemic apparently brings structure-breaking shocks to most of the components in five-year bid-ask spreads as shown in Figure 11. Although the shock to the adverse selection from buy side increases l_A's cross-sectional dispersion on the outset, it pushes down l_A as the pandemic develops (the left subplot on the first row in Panel (b) of Figure 11). This makes intuitive sense, as most CDS buyers during the pandemic are expected to be driven by general concerns instead of insider information. In contrast, the adverse selection from the sell side (l_B) increases dramatically after an initial drop at the beginning of the pandemic (the middle subplot on the first row in Panel (b) of Figure 11). This is also understandable: one would be suspicious of

[3]Duffie and Zhu (2011) show that the expected counterparty exposures and collateral demands are lower when clearing on the same CCP than on different ones. The current CDS market structure with the Depository Trust & Clearing Corporation (DTCC) being the only CCP is consistent with Duffie and Zhu (2011)'s recommendation.

having insider information if they are willing to sell CDS despite the heightened uncertainty during the pandemic.

The shocks to the monopolist profits (γ_A) and the counterparty risk from sell side (γ_B) increase both the cross-sectional dispersion and the level of these two components. The uncertainty brought by the pandemic increases the demand for default insurance. The higher demand naturally translates into higher monopolist profits for the dealers, which are clearly reflected in the increased γ_A (the left subplot on the second row in Panel (b) of Figure 11). At the same time, the uncertainty also increases the counterparty risk which shows up in the increased γ_B (the middle subplot on the second row in Panel (b) of Figure 11). The counterparty risk is a primary concern for investors during the 2007 - 2009 financial crisis (Bai and Collin-Dufresne, 2019), our results show that this is also true during the COVID-19 pandemic. Studying the large margin calls issued by the CCPs, Huang and Takáts (2020) also document heightened counterparty risks during the pandemic.

The recovery-related liquidity component (η) also deepens due to the pandemic in absolute terms (the right subplot on the first row in Panel (a) of Figure 11). However, in relative terms η accounts for fewer weights in the bid-ask spread during the pandemic (the right subplot on the first row in Panel (b) of Figure 11). η is a component related to the corporate bond market. The fact that the corporate bond market component weights less in the bid-ask spread during the pandemic shows that the CDS market-specific uncertainty due to the pandemic makes the CDS market less competitive, which is reflected in the higher monopolist profits, and brings more informational friction, which is reflected in the more concerns for the adverse selection from sell side and the counterparty risk.

5.3 CDS Bid-ask spreads and market wide liquidity

The CDS market functions as an "insurance" market for the corporate bonds (Jarrow, 2011). This cross market nature renders a channel connecting the bid-ask spreads in the CDS market with market-wide liquidity risk factors. This channel is confirmed by the results in the second

column of Table 2 where the weekly changes of five-year bid-ask spreads are regressed to the weekly changes of the NOISE liquidity measure due to Hu, Pan, and Wang (2013). We can see that the coefficients of both contemporaneous and lagged changes in the NOISE are significantly positive. To further examine which components of the bid-ask spreads explain the channel, we also regress their weekly changes to the weekly changes of the NOISE. The results are presented in the columns three to eight and show that among all components, l_A, η, and λ explain the channel.

[*Insert Table 2 about here*]

As stated in Hu, Pan, and Wang (2013), the NOISE liquidity factor inversely measures the scarcity of the overall arbitrage capital available in the market. When the market illquidity is high, the buy side adverse selection decreases as less arbitrage capital is available. This reverse relation is captured by the significantly negative coefficients of the lagged weekly change of the NOISE in the third column of Table 2. By construction, η is designated to capture the illiquidity of the defaulted corporate bond market which is naturally expected to be positively related to the market-wide liquidity risk factor. The significantly positive coefficients of both contemporaneous and lagged weekly change of the NOISE in the fifth column in Table 2 confirm that the calibrated η using our model is indeed able to capture the liquidity information from outside the CDS market.

From the last column in Table 2, we also find that the lagged weekly change of NOISE is significantly and positively correlated with the weekly change of λ. Chen et al. (2018) and Chun et al. (2019) show that there is a clear interaction between default and liquidity risks in both the corporate bond and the municipal bond markets. Consistent with their results, the positive correlation between the NOISE and the default component λ observed here indicates the interaction also exists in the CDS market. Considering that η and λ are also noticeable components in the mid-CDS quotes (see Section 4.2), the fact that η and λ are positively correlated with the NOISE is consistent with the notion that liquidity risk is priced in the cross section of returns on CDS (Junge and Trolle, 2015).

5.4 Predictive analysis on adverse selection

Among all the components, it is well-known that the adverse information cost due to adverse selection from the buyer and seller has predictive power on the expected equilibrium price. Due to the existence of insider traders with superior information, a sale to the dealer conveys information that causes the dealer to revise the expected equilibrium price. This idea has been articulated in Stoll (1989).

5.4.1 Short term predictive power

Under our framework, we expect the lagged change in the adverse selection from the buy (sell) side, Δl_A (Δl_B) positively (negatively) predicts short term changes in the mid-quote, which we assume presents the expected CDS premium. Keeping in mind these expectations, we run the following dynamic daily panel regression using the five-year CDS mid quote as the LHS variable:

$$\Delta mid_{t,i}(5yr) = c_{t,i} + a\Delta\bar{l}_{A,t-1,i} + b\Delta\bar{l}_{B,t-1,i} + controls + \epsilon_{t,i} \tag{4}$$

where Δ is the difference operator; $mid_{t,i}$ is the mid quote; *controls* are the control variables and include $\Delta\eta_{t-1,i}$, $\Delta\overline{\gamma}_{A,t-1,i}$, $\Delta\overline{\gamma}_{B,t-1,i}$, $\Delta\lambda_{t-1,i}$, and $\Delta BAS_{t-1,i}(5yr)$; $\epsilon_{t,i}$ is the error term; the overline indicates the variables are the average cross the values at one-year, five-year and 10-year.

The full sample regression results are presented in the second column of Table 3a. We can see that $\Delta\bar{l}_{A,t-1,i}$ and $\Delta\bar{l}_{B,t-1,i}$ have significant predictive power on $\Delta mid_{t,i}$. Consistent with our expectation, $\Delta\bar{l}_{A,t-1,i}$'s significantly positive coefficient indicates that the adverse selection from the buy side predicts the future change in the mid quote: when the adverse selection from the buy side increases, the dealers are likely to adjust their ask price upwards the next day. Ceteris paribus, the next day's mid price will increase. A similar explanation applies to $\Delta\bar{l}_{B,t-1,i}$ which has an significantly negative coefficient: when the adverse selection from the sell side increases, the next day's bid price is likely to decrease, so is the next day's mid price.

To further investigate whether this predictive power behaves differently in different credit rating groups, we run the regressions by ratings. The results of the top rating group (AAA, AA, A: 35% of the full sample) are presented in Table 3b, those of the mid rating group (BBB and BB: 43% of the full sample) are in Table 3c, and those of the low rating group (B, CCC, and D: 22% of the full sample) are in Table 3d. Indeed, we find that the significantly negative predictive power of $\Delta\bar{l}_{B,t-1,i}$ comes mainly from the top and mid rating group, while the significantly positive predictive power of $\Delta\bar{l}_{A,t-1,i}$ comes from the low rating groups. This observation indicates that the adverse selection from sell (buy) side is more informative about future quote direction among high (low) credit ratings firms.

[*Insert Table 3 about here*]

5.4.2 Explanatory power on cross-sectional returns

For simplicity, we follow Das, Hanouna, and Sarin (2009), Fabozzi, Giacometti, and Tsuchida (2016), and Pelster and Vilsmeier (2018), and use log-returns (log difference of the mid quotes) of the five-year CDS premium to approximate the returns from trading five-year CDS contracts. We conduct a double sorting excise to investigate the explanatory power of the bid-ask spread components on the cross-sectional CDS log-returns.

Specifically, at each month end (formation month), we first sort all firms into three groups: the low, mid, and high, based on the the monthly average mid quotes within the month. These are our first level groups. In the second level sorting we use BAS and the percentage components of BAS as sorting variables. The firms within each first level group are further sorted into three subgroups by the monthly average of one second level sorting variable within the month. Therefore, in each first level group, there are three portfolios (low, mid, high). These portfolios are held for one month and we record the equal weighted log-returns of these portfolios from the next month. We repeat the procedure and rebalance the portfolios on a monthly basis. The time series averages of the High-minus-Low (HmL) returns with their t-test significance in the first level groups are presented in Table 4.

[*Insert Table 4 about here*]

The results in Table 4 clearly demonstrate the benefits of our model decomposition for the CDS bid-ask spreads. When the BAS is used as the second sorting variable, none of the HmL returns are significant (see the second row of Table 4). The returns are much more promising when the adverse selection components are used as the second sorting variable. For example, shown in the third and fourth rows of Table 4, when sorted by l_A (l_B), the full sample HmL portfolio generates a monthly return of 0.6% (-1%) with t-statistic of 1.7 (-1.8). When $l_A - l_B$ is used as the second sorting variable (see the fifth row of Table 4), the full sample HmL portfolio generates a even higher and more significant monthly return of 1.2% with t-statistic of 2.3. These results indicate that the adverse selection components identified from the CDS bid-ask spreads using our model provide useful information beyond the bid-ask spreads per se. Together with the results in Table 3, we show that the adverse selection components not only have short term time series predictive power on the mid quotes, but not have significant cross-sectional explanatory power on the returns.

It is also worth noting that when sorted by the percentage component γ_A, the HmL portfolio generates a significant monthly return of -1.2% with t-statistic of -2.7. It is interesting that the sign of the return is opposite to that of the γ_A coefficient in Table 3b. This could mean that γ_A captures a transitional uncertainty component in the CDS bid-ask spreads which introduces an overpricing on the CDS pricing (see, e.g., Cai, Ye, and Zhao, 2020; Duffie and Lando, 2001; Yu, 2005) but with only a short-term effect. The CDS premium converts when the informational friction is resolved, therefore results in lower returns in longer periods.

Although the full sample results are significant for l_A, l_B, and γ_A, the explanatory power comes exclusively from the low CDS mid quote group (compare the third column to the fourth and fifth columns in Table 4). This means the bid-ask quotes for low credit risk firms have better informational content for CDS asset pricing than those for high credit risk firms.

5.5 Adverse selection - induced inventory costs

As mentioned in Section 2.3.3, l_A and l_B are the net effect of adverse selection and inventory costs. Although their positive calibrated values show that the adverse selection dominates the inventory costs, it is interesting to investigate whether the adverse selection - induced inventory costs are significant. Their significance can be tested by regressing the changes of the bid (ask) price to the changes of l_A (l_B). If the inventory costs are insignificant, then we should observe insignificant coefficient for Δl_A in the bid price regression and insignificant coefficient for Δl_B in the ask price regression. They are significant otherwise. These regressions can be conducted by simply replacing the LHS of (4) with $\Delta ask_{t,i}(5yr)$ and $\Delta bid_{t,i}(5yr)$. The regression results are presented in the third and fourth columns in Table 3a. The coefficient of l_A (l_B) is significant in the bid (ask) regression. These results confirm that the adverse selection - induced inventory costs also have significantly predictive power. We now present a regression-based approach to quantify them.

From Section 2.3.3, we know $l_A = l_A^0 - \beta l_B^0$ and $l_B = l_B^0 - \alpha l_A^0$. These two equations can be rewritten as

$$l_A = (1 - \alpha\beta) l_A^0 - \beta l_B;$$
$$l_B = (1 - \alpha\beta) l_B^0 - \alpha l_A.$$

Given the calibrated l_A and l_B at the different horizons, α and β can be estimated using linear panel regressions controlled for the firm fixed effect and time fixed effect. Table 5 presents the regression results. From the table we can see α is significant at the one-, five-, seven-, and 10-year maturities. The significance of β is similar except that β is insignificant at the five-year maturity. On average, the coefficients are higher at the one-year horizon. This indicates that the inventory costs are higher when the CDS contracts are near maturity.

[*Insert Table 5 about here*]

Given α and β, l_A^0 and l_B^0 can be computed using the following system of equations:

$$\begin{bmatrix} l_A \\ l_B \end{bmatrix} = \begin{bmatrix} 1 & -\beta \\ -\alpha & 1 \end{bmatrix} \begin{bmatrix} l_A^0 \\ l_B^0 \end{bmatrix} \Longrightarrow \begin{bmatrix} l_A^0 \\ l_B^0 \end{bmatrix} = \begin{bmatrix} 1 & -\beta \\ -\alpha & 1 \end{bmatrix}^{-1} \begin{bmatrix} l_A \\ l_B \end{bmatrix}.$$

Specifically, we quantify the inventory cost in terms of the bid-ask spread differences due to αl_A^0 and βl_B^0. Their distributions are plotted in Figure 12. Figure 12 shows that from the dealer's perspective, the sell side induced inventory costs βl_B^0 are generally higher than the buy side ones. This is consistent with the common sense that in normal circumstances the need for hedge is stronger when the dealer is paying CDS premiums than when receiving premiums, as the urgency for balancing the cash flows is stronger in the former. The term structure distributions in panel (a) of Figure 12 also confirm that the inventory costs are mostly on short and long (non-standard) maturity contracts, with the shorter maturity contracts having higher inventory costs than the longer maturity ones, in other words, the dealers are more willing to narrow the bid-ask spreads at the shorter maturities for hedging purposes.

From the time series distributions in panel (b) of Figure 12, we can see that before the COVID-19 pandemic the buy side adverse selection induced inventory costs αl_A^0 have narrower distributions over time than the sell side ones βl_B^0. Also the median value of βl_B^0 drops significantly after 2013 before 2020, indicating that in the recent years the sell side adverse selection induced inventory costs have gone down. Similar to the case of other components, the outbreak of pandemic brings an acute and positive shock to the dynamics of the inventory costs. Both buy side and sell side induced inventory costs shoot up and come back rapidly in March and April 2020. The cross-sectional dispersion also bursts during this period. The impact on the buy side induced inventory costs seems significantly bigger than the sell side. This shows that the dealers perceive the pandemic as an extraordinary circumstance where the need for hedge has become stronger when receiving premiums than when paying premiums due to heightened default risks. These observations during the pandemic indicates that the CDS dealers are highly risk-averse when facing radical uncertainty.

[*Insert Figure 12 about here*]

6 Conclusions

In this paper, we develop a reduced-form CDS pricing model with analytical solutions that quantify CDS bid-ask spreads into different components, namely, adverse selection, monopolist profits, inventory costs, LGD, and counterparty risk. An important feature of our study is the use of a large number of single name CDS bid-ask quotes data. The analytical nature of our model makes the large scale computation tractable.

Our empirical results show that the recovery-related liquidity component accounts for a large part of the bid-ask spreads, especially during normal times. The adverse selection components also account for a sizeable portion in non-five-year CDS quotes, with the sell (buy) side concentrated on the shorter (longer) maturities. The sell buy component is significantly larger than the buy side one. Consistent with the traditional literature on bid-ask spreads, changes in the averse selection components predict future changes in the CDS premiums.

The monopolist profits component is slightly smaller in size than the adverse selection components, but concentrated mostly on the mid maturities around five-year. It is also important to note that during the COVID-19 pandemic, the counterparty risk component, which has historically been small, shoot up noticeably. So do the adverse selection from the sell side and the monopolist profits, indicating that the pandemic makes the CDS market less competitive and efficient.

Overall, our study offers a new tool for analyzing the CDS bid-ask spreads, the key aspect of the liquidity of the CDS market. We hope our pioneer work will bring more research interests to studying the liquidity issues in the CDS market and help the long-run development of the CDS market.

References

Acharya, Viral V and Timothy C Johnson (2007). "Insider trading in credit derivatives". In: *Journal of Financial Economics* 84.1, pp. 110–141.

Affleck-Graves, John, Shantaram P Hegde, and Robert E Miller (1994). "Trading mechanisms and the components of the bid-ask spread". In: *The Journal of Finance* 49.4, pp. 1471–1488.

Aldasoro, Iñaki and Torsten Ehlers (2018). "The credit default swap market: what a difference a decade makes". In: *BIS Quarterly Review, June*.

Altman, E.I., B. Brady, A. Resti, and A. Sironi (2005). "The Link between Default and Recovery Rates: Theory, Empirical Evidence, and Implications". In: *The Journal of Business* 78.6, pp. 2203–2228.

Amihud, Yakov and Haim Mendelson (1986). "Asset pricing and the bid-ask spread". In: *Journal of financial Economics* 17.2, pp. 223–249.

— (1989). "The effects of beta, bid-ask spread, residual risk, and size on stock returns". In: *The Journal of Finance* 44.2, pp. 479–486.

Arce, Óscar, Javier Gonzalez Pueyo, and Lucio Sanjuán (2010). *The Credit Default Swaps market: areas of vulnerability and regulatory responses*. Working Paper. CNMV.

Arora, Navneet, Priyank Gandhi, and Francis A Longstaff (2012). "Counterparty credit risk and the credit default swap market". In: *Journal of Financial Economics* 103.2, pp. 280–293.

Bai, Jennie and Pierre Collin-Dufresne (2019). "The CDS-bond basis". In: *Financial Management* 48.2, pp. 417–439.

Bongaerts, Dion, Frank De Jong, and Joost Driessen (2011). "Derivative pricing with liquidity risk: Theory and evidence from the credit default swap market". In: *The Journal of Finance* 66.1, pp. 203–240.

Cai, Charlie X, Xiaoxia Ye, and Ran Zhao (2020). "Informational Friction, Economic Uncertainty and CDS-Bond Basis". In: *Available at SSRN 3746637*.

Chen, Hui, Rui Cui, Zhiguo He, and Konstantin Milbradt (2018). "Quantifying liquidity and default risks of corporate bonds over the business cycle". In: *The Review of Financial Studies* 31.3, pp. 852–897.

Chen, Jiakai, Haoyang Liu, Asani Sarkar, and Zhaogang Song (2021). "Dealers and the Dealer of Last Resort: Evidence from MBS Markets in the COVID-19 Crisis". In: *Federal Reserve Bank of New York Staff Reports* 933.

Chun, Albert Lee, Ethan Namvar, Xiaoxia Ye, and Fan Yu (2019). "Modeling municipal yields with (and without) bond insurance". In: *Management Science* 65.8, pp. 3694–3713.

Collin-Dufresne, Pierre, Benjamin Junge, and Anders B Trolle (2020). "Market structure and transaction costs of index CDSs". In: *The Journal of Finance* 75.5, pp. 2719–2763.

Das, Sanjiv R, Paul Hanouna, and Atulya Sarin (2009). "Accounting-based versus market-based cross-sectional models of CDS spreads". In: *Journal of Banking & Finance* 33.4, pp. 719–730.

Deventer, Donald R. van (2012). *The Credit Default Swap Market and Anti-Trust Considerations*. Online Article. Kamakura Blog.

Du, Songzi and Haoxiang Zhu (2017). "Are CDS auctions biased and inefficient?" In: *The Journal of Finance* 72.6, pp. 2589–2628.

Duffie, D. and D. Lando (2001). "Term structures of credit spreads with incomplete accounting information". In: *Econometrica*, pp. 633–664.

Duffie, D., J. Pan, and K. Singleton (2000). "Transform analysis and asset pricing for affine jump-diffusions". In: *Econometrica*, pp. 1343–1376.

Duffie, Darrell (1999). "Credit swap valuation". In: *Financial Analysts Journal* 55.1, pp. 73–87.

Duffie, Darrell, Lasse Heje Pedersen, and Kenneth J Singleton (2003). "Modeling sovereign yield spreads: A case study of Russian debt". In: *The journal of finance* 58.1, pp. 119–159.

Duffie, Darrell and Haoxiang Zhu (2011). "Does a central clearing counterparty reduce counterparty risk?" In: *The Review of Asset Pricing Studies* 1.1, pp. 74–95.

Fabozzi, Frank J, Rosella Giacometti, and Naoshi Tsuchida (2016). "Factor decomposition of the Eurozone sovereign CDS spreads". In: *Journal of International Money and Finance* 65, pp. 1–23.

Glosten, Lawrence R (1989). "Insider trading, liquidity, and the role of the monopolist specialist". In: *Journal of Business*, pp. 211–235.

Glosten, Lawrence R and Lawrence E Harris (1988). "Estimating the components of the bid/ask spread". In: *Journal of financial Economics* 21.1, pp. 123–142.

Glosten, Lawrence R and Paul R Milgrom (1985). "Bid, ask and transaction prices in a specialist market with heterogeneously informed traders". In: *Journal of financial economics* 14.1, pp. 71–100.

Haddad, Valentin, Alan Moreira, and Tyler Muir (2020). "When selling becomes viral: Disruptions in debt markets in the covid-19 crisis and the Fed's response". In: *Review of Financial Studies*, forthcoming.

Hu, Grace Xing, Jun Pan, and Jiang Wang (2013). "Noise as information for illiquidity". In: *The Journal of Finance* 68.6, pp. 2341–2382.

Huang, Roger D and Hans R Stoll (1997). "The components of the bid-ask spread: A general approach". In: *The Review of Financial Studies* 10.4, pp. 995–1034.

Huang, Wenqian and Előd Takáts (2020). *The CCP-bank nexus in the time of Covid-19*. Tech. rep. Bank for International Settlements.

Jarrow, Robert, Haitao Li, Xiaoxia Ye, and May Hu (2018). "Exploring mispricing in the term structure of CDS spreads". In: *Review of Finance* 23.1, pp. 161–198.

Jarrow, Robert A (2011). "The economics of credit default swaps". In: *Annu. Rev. Financ. Econ.* 3.1, pp. 235–257.

Jarrow, Robert A and Fan Yu (2001). "Counterparty risk and the pricing of defaultable securities". In: *The Journal of Finance* 56.5, pp. 1765–1799.

Junge, Benjamin and Anders B Trolle (2015). "Liquidity risk in credit default swap markets". In: *Swiss Finance Institute Research Paper* 13-65.

Lin, Ji-Chai, Gary C Sanger, and G Geoffrey Booth (1995). "Trade size and components of the bid-ask spread". In: *The Review of Financial Studies* 8.4, pp. 1153–1183.

Longstaff, F.A., S. Mithal, and E. Neis (2005). "Corporate yield spreads: Default risk or liquidity? New evidence from the credit default swap market". In: *Journal of Finance* 55.5, pp. 2213–2253.

Loon, Yee Cheng and Zhaodong Ken Zhong (2014). "The impact of central clearing on counterparty risk, liquidity, and trading: Evidence from the credit default swap market". In: *Journal of Financial Economics* 112.1, pp. 91–115.

— (2016). "Does Dodd-Frank affect OTC transaction costs and liquidity? Evidence from real-time CDS trade reports". In: *Journal of Financial Economics* 119.3, pp. 645–672.

Meng, Qiang, Amnon Levy, Andrew Kaplin, Yashan Wang, and Zhenya Hu (2010). "Implications of PD-LGD correlation in a portfolio setting". In: *Moody?s Analytics*.

Menyah, Kojo and Krishna Paudyal (2000). "The components of bid–ask spreads on the London stock exchange". In: *Journal of Banking & Finance* 24.11, pp. 1767–1785.

Oehmke, Martin and Adam Zawadowski (2017). "The anatomy of the CDS market". In: *The Review of Financial Studies* 30.1, pp. 80–119.

Pelster, Matthias and Johannes Vilsmeier (2018). "The determinants of CDS spreads: evidence from the model space". In: *Review of Derivatives Research* 21.1, pp. 63–118.

Stoll, Hans R (1989). "Inferring the components of the bid-ask spread: Theory and empirical tests". In: *the Journal of Finance* 44.1, pp. 115–134.

Tang, Dragon Yongjun and Hong Yan (2017). "Understanding transactions prices in the credit default swaps market". In: *Journal of Financial Markets* 32, pp. 1–27.

Yu, Fan (2005). "Accounting transparency and the term structure of credit spreads". In: *Journal of financial economics* 75.1, pp. 53–84.

Figure 1: An example of the term structure of bid-ask spreads

The figure shows the distribution of T-Mobile USA Inc's bid-ask spread term structure over September 2013 to November 2020 (daily data). The maturities include six-month, one- to five-year, seven-year and 10-year. The unit of the y-axis is basis-point. Mean and median along with 95 and five percentiles are plotted.

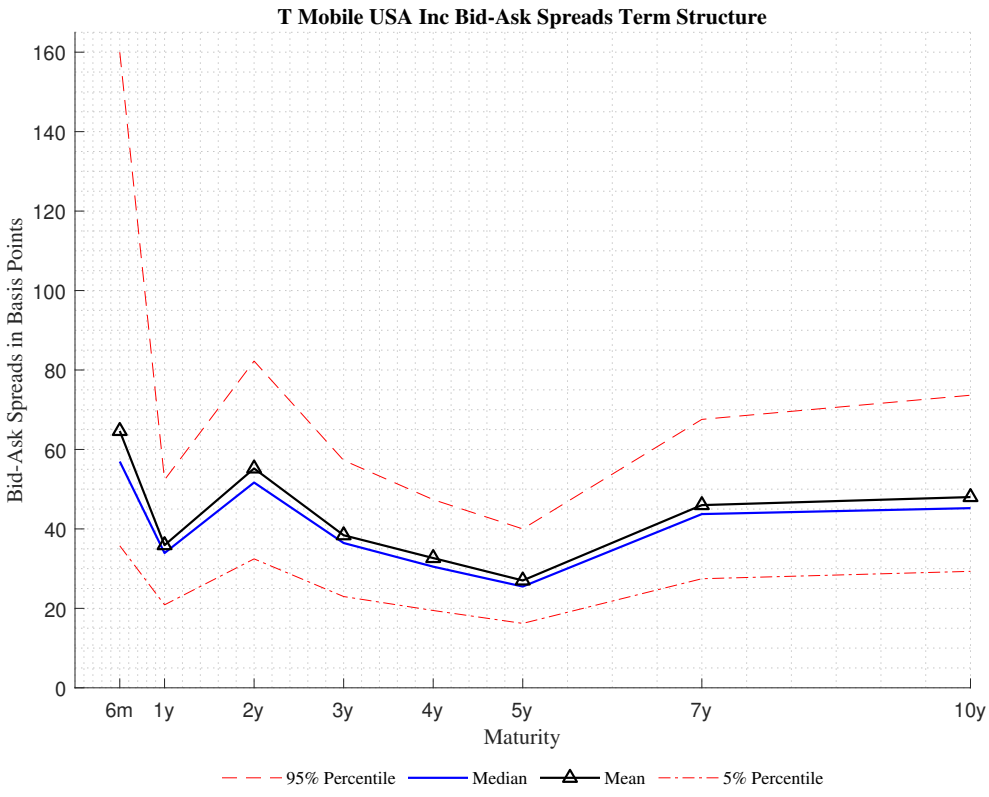

Figure 2: Time series of average CDS mid-quotes and bid-ask spreads

From the left to the right, the panels plot time series of the bid-ask spreads, CDS mid-quotes, and relative spreads (defined as bid-ask / CDS mid-quote), respectively. In each panel three maturities are included: one-year, five-year, and 10-year. The sample period covers November 2011 to November 2020. The unite of the y-axis in the left and middle panels is basis-point, and it is percent in the right panel.

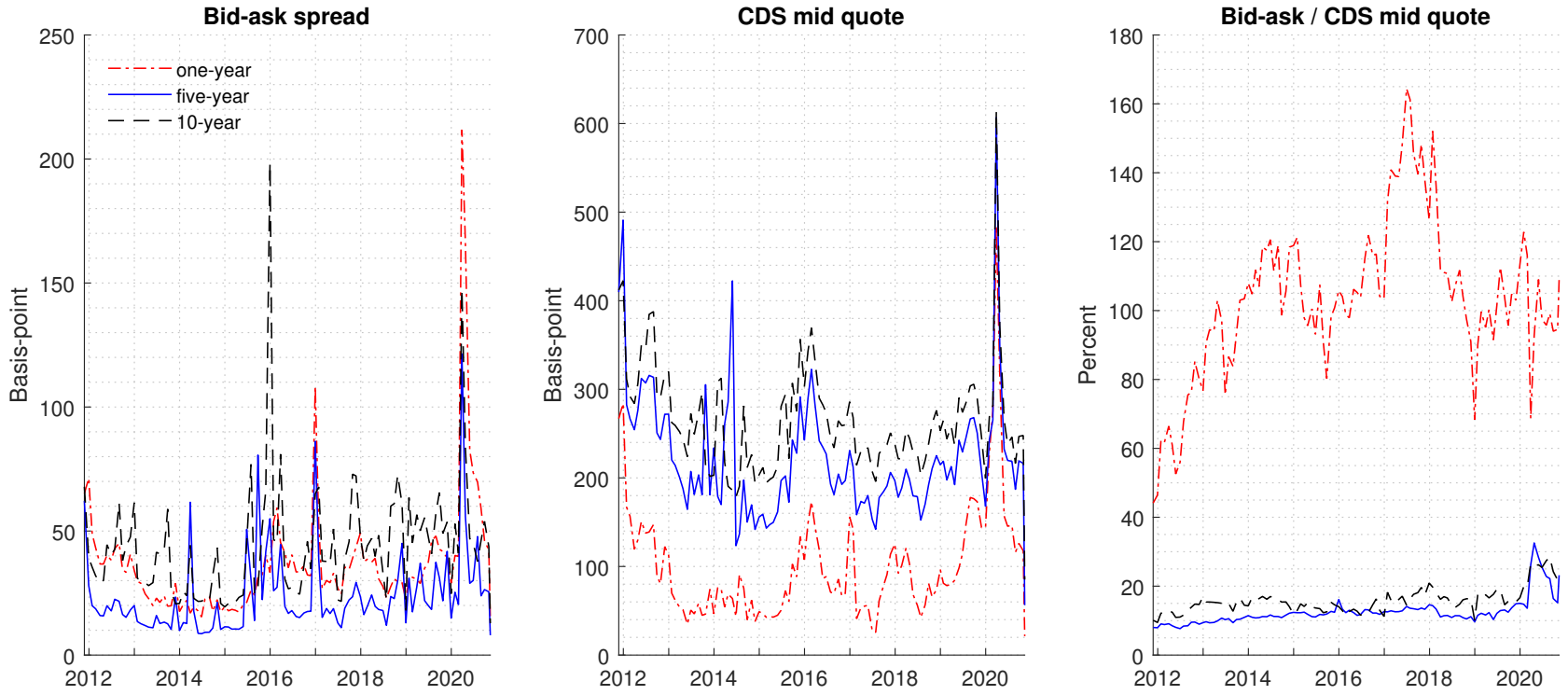

Figure 3: Time series plots of average weekly notional

From the left to the right, the panels plot time series of the weekly transacted gross notional, weekly net notional outstanding, and weekly average notional per contract, respectively. The lines aggregate figures across all maturities. The sample period covers November 2011 to November 2020. The unite of the y-axis in the left and middle panels is billion USD, and it is million USD in the right panel.

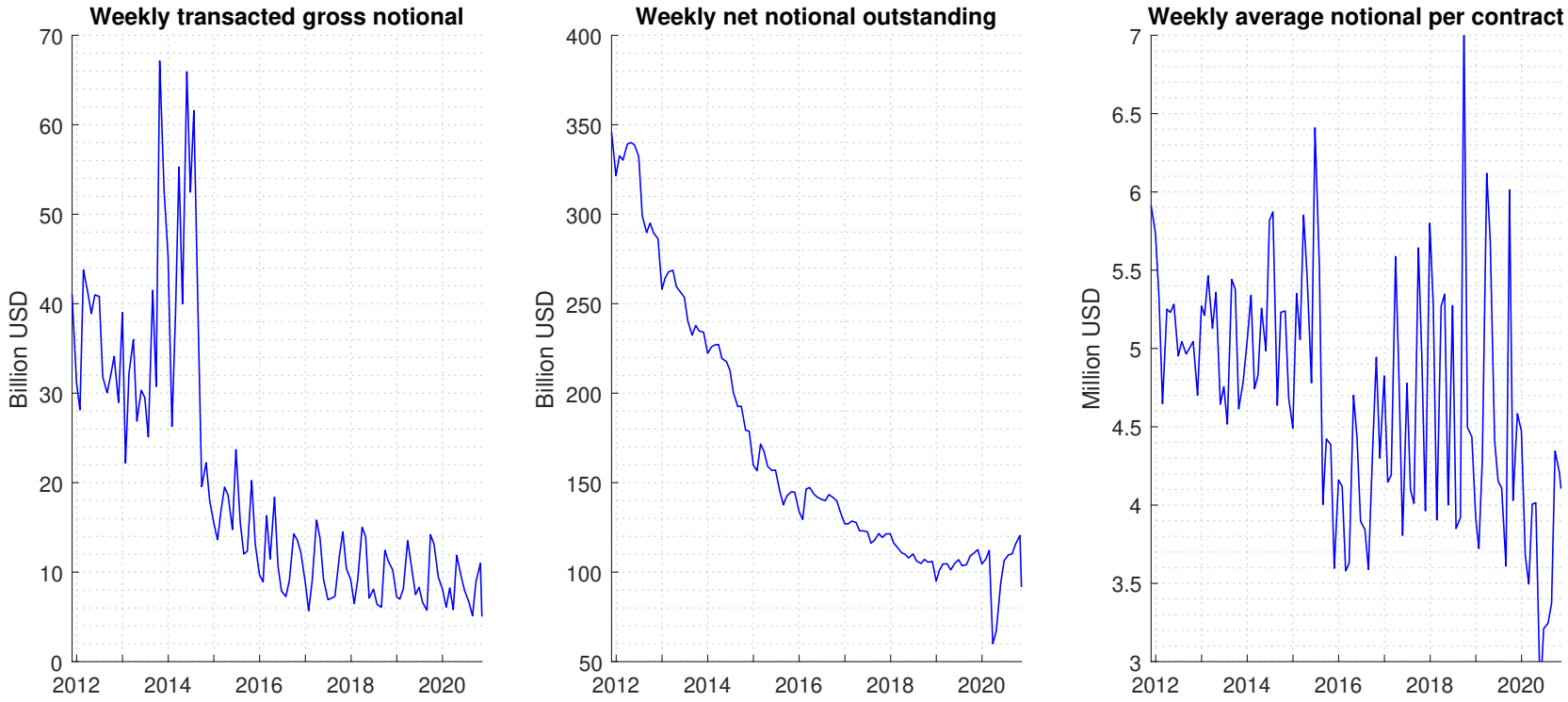

Figure 4: Term structure evolution of T-Mobile USA Inc's data

The left and right panels show the the term structure evolution over September 2013 to November 2020 for T-Mobile USA Inc's CDS mid-quotes and bid-ask spreads, respectively. The maturities include one- to five-year, seven-year and 10-year. The unit of the y-axis in both panels is basis-point.

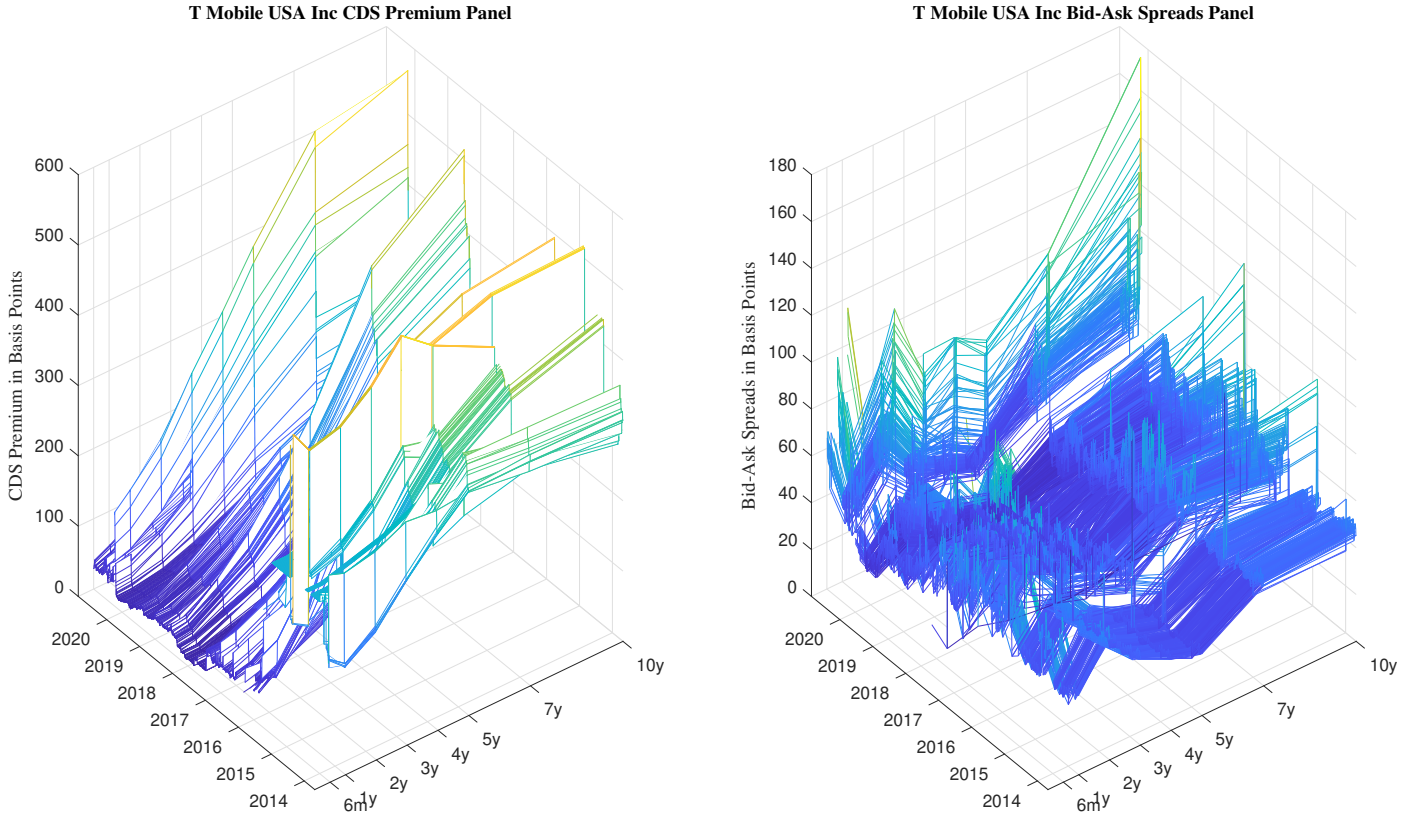

Figure 5: Fitted model vs actual data: T-Mobile USA Inc

The a) and b) panels compare the respective model results with the time-series average of T-Mobile USA Inc's CDS mid-quote (panel a) and bid-ask spreads (panel b), to which the model is calibrated. The actual data are in dash-dot lines and the model results are in solid lines. The time-series average is based on daily data over September 2013 to November 2020. The maturities include six-month, one- to five-year, seven-year and 10-year. The unit of the y-axis in both panels is basis-point.

a) CDS premium

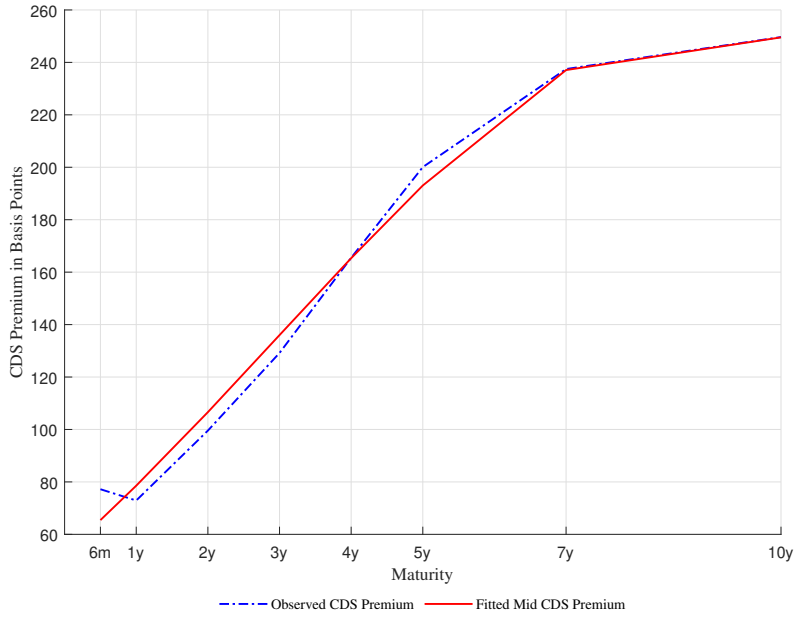

b) Bid-Ask Spreads

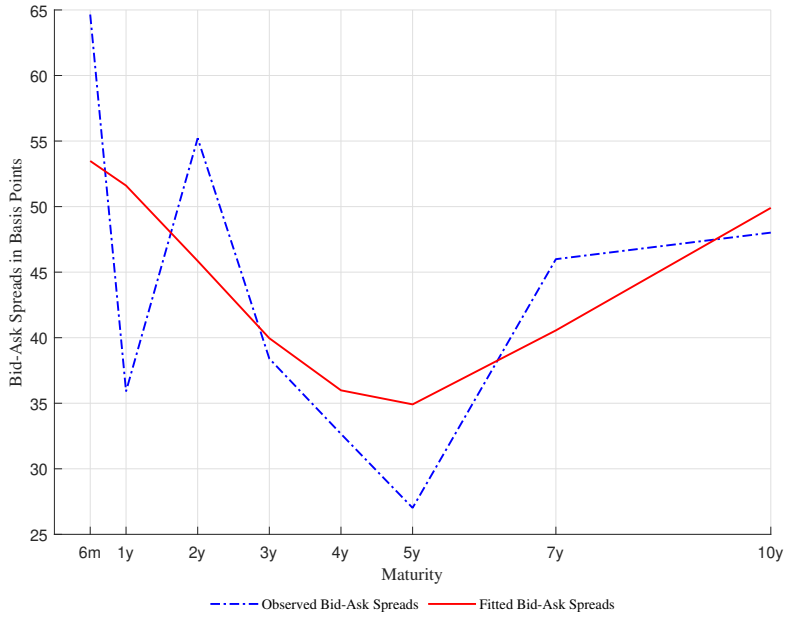

Figure 6: Decomposition of the bid-ask spread: T-Mobile USA Inc

The left (right) panel presents the various components in T-Mobile USA Inc's bid-ask spread separately (cumulatively) across maturities ranging from six-month to 10-year. For benchmarking purpose, the baseline bid-ask spread is also plotted in the left panel (the light blue line). These components are adverse selection from buy side (the blue line/area), adverse selection from sell side (the red line/area), recovery-related liquidity (the yellow line/area), monopolist profits (the purple line/area), and counterparty risk (the green line/area). The unit of the y-axis in both panels is basis-point.

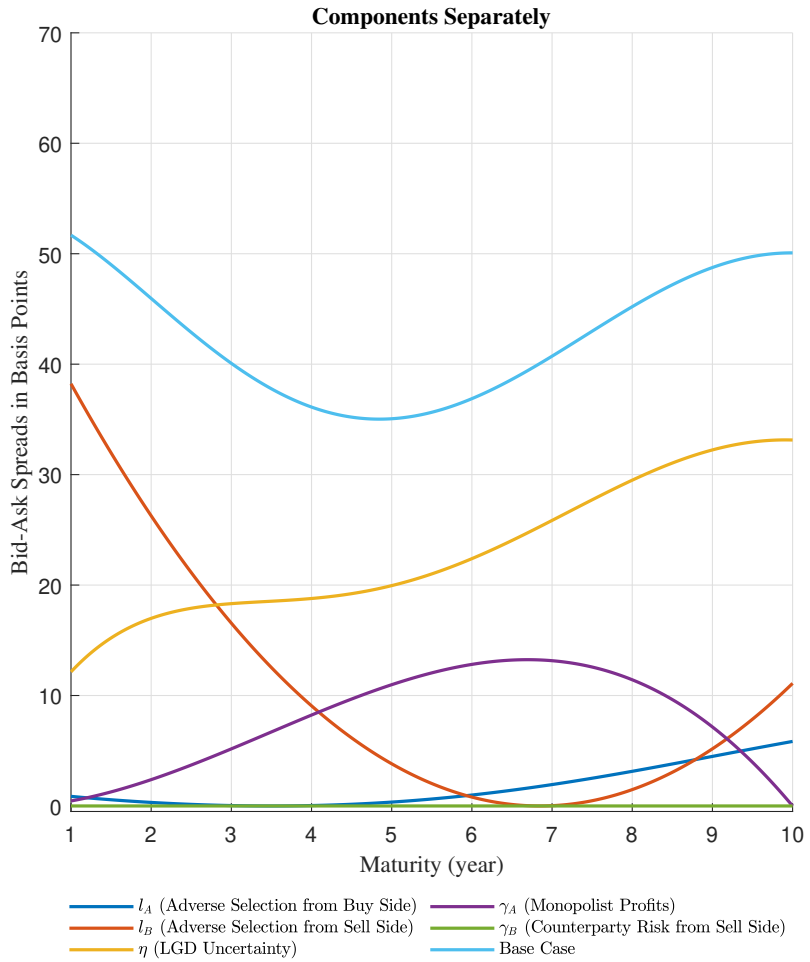

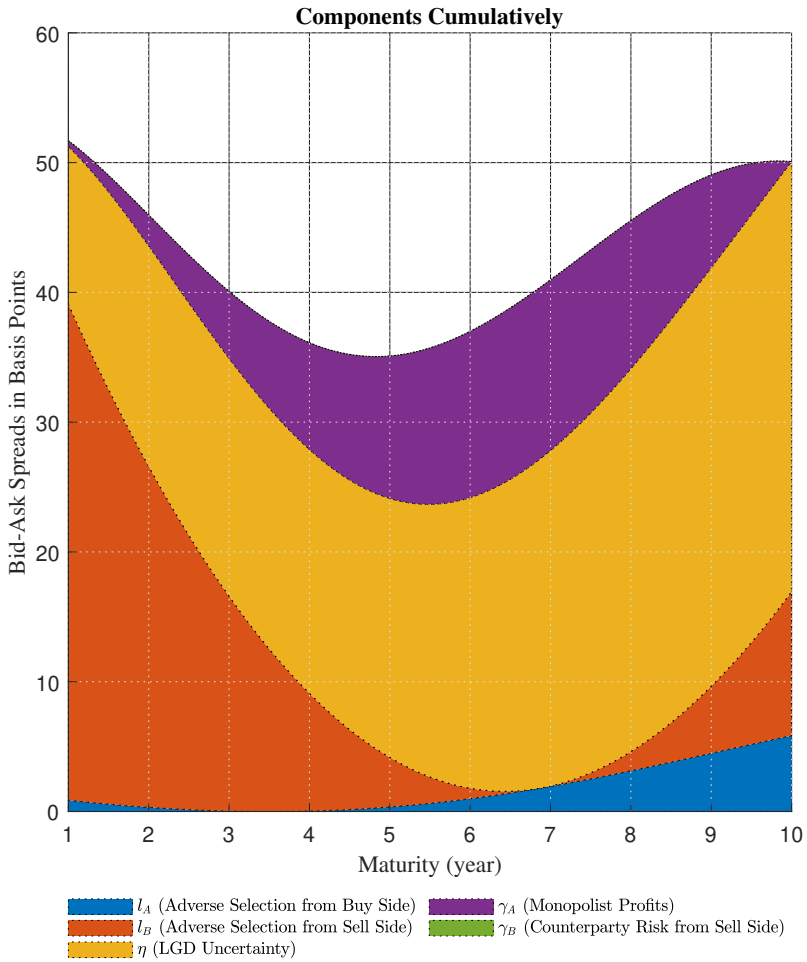

Figure 7: Time series of components in the bid-ask spread: T-Mobile USA Inc

The upper panel presents the time series of the various components (averaging across the maturities) in T-Mobile USA Inc's bid-ask spread in absolute terms. The lower panel presents the time series of the components in relative terms with respect to the baseline bid-ask spread averaging across the maturities. For benchmarking purpose, the baseline bid-ask spread is also plotted in the upper panel (the light blue line). These components are adverse selection from buy side (the blue line), adverse selection from sell side (the red line), recovery-related liquidity (the yellow line), monopolist profits (the purple line), and counterparty risk (the green line). The unit of the y-axis in the upper (lower) panel is basis-point (percent).

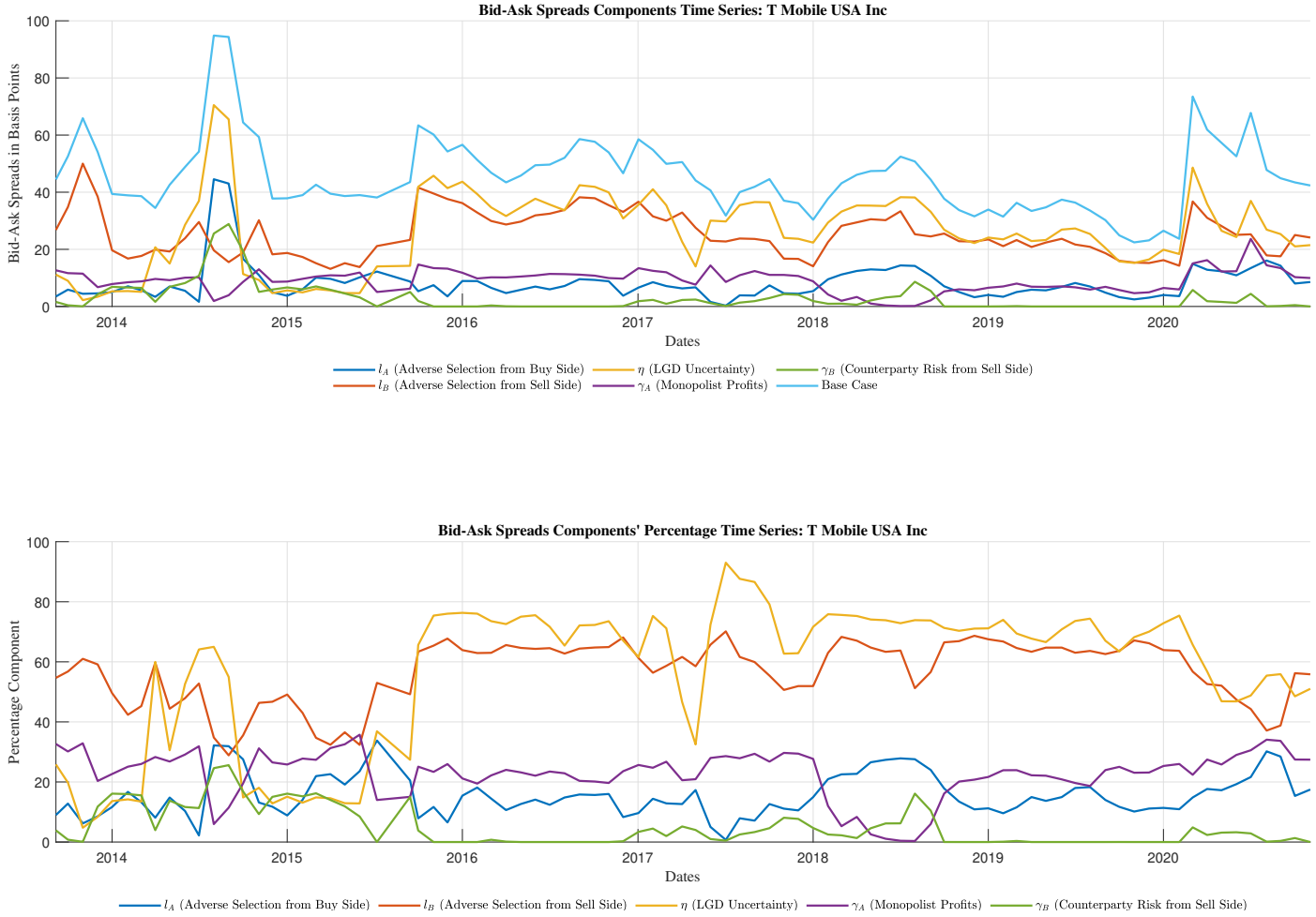

Figure 8: Decomposition of the CDS mid-quote: T-Mobile USA Inc

The figure presents the various components in T-Mobile USA Inc's CDS mid-quote separately across maturities ranging from six-month to 10-year. These components are adverse selection from buy side (the blue line), adverse selection from sell side (the red line), recovery-related liquidity (the yellow line), monopolist profits (the purple line), counterparty risk (the green line), and default risk (the light blue line). The unit of the y-axis is basis-point.

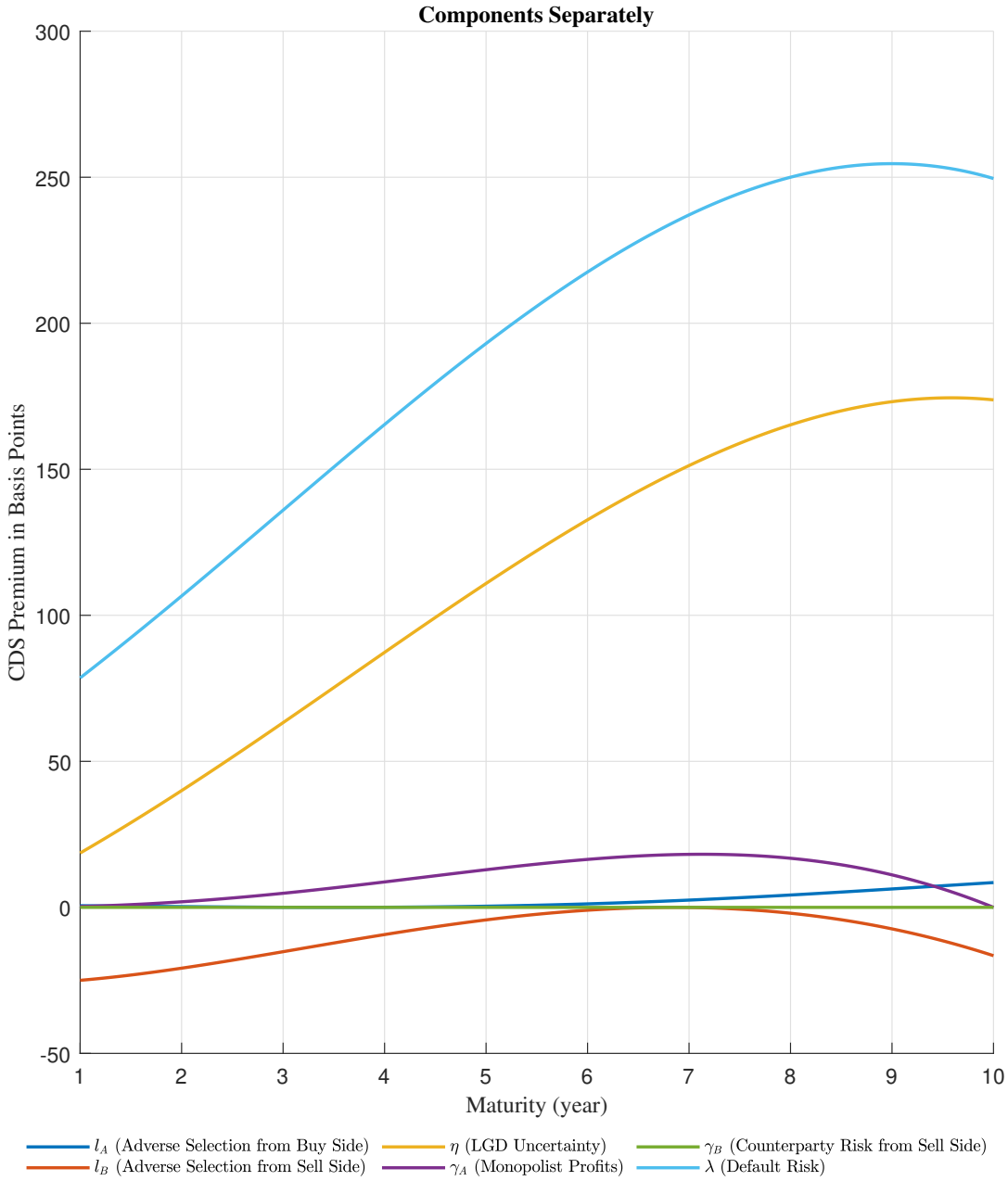

Figure 9: Time series of components in the CDS mid-quote: T-Mobile USA Inc

The upper panel presents the time series of the various components (averaging across the maturities) in T-Mobile USA Inc's CDS mid-quote in absolute terms. The lower panel presents the time series of the components in relative terms with respect to the CDS mid-quote averaging across the maturities. For benchmarking purpose, the baseline CDS mid-quote is also plotted in the upper panel (the light blue line). These components are adverse selection from buy side (the blue line), adverse selection from sell side (the red line), recovery-related liquidity (the yellow line), monopolist profits (the purple line), and counterparty risk (the green line). The unit of the y-axis in the upper (lower) panel is basis-point (percent).

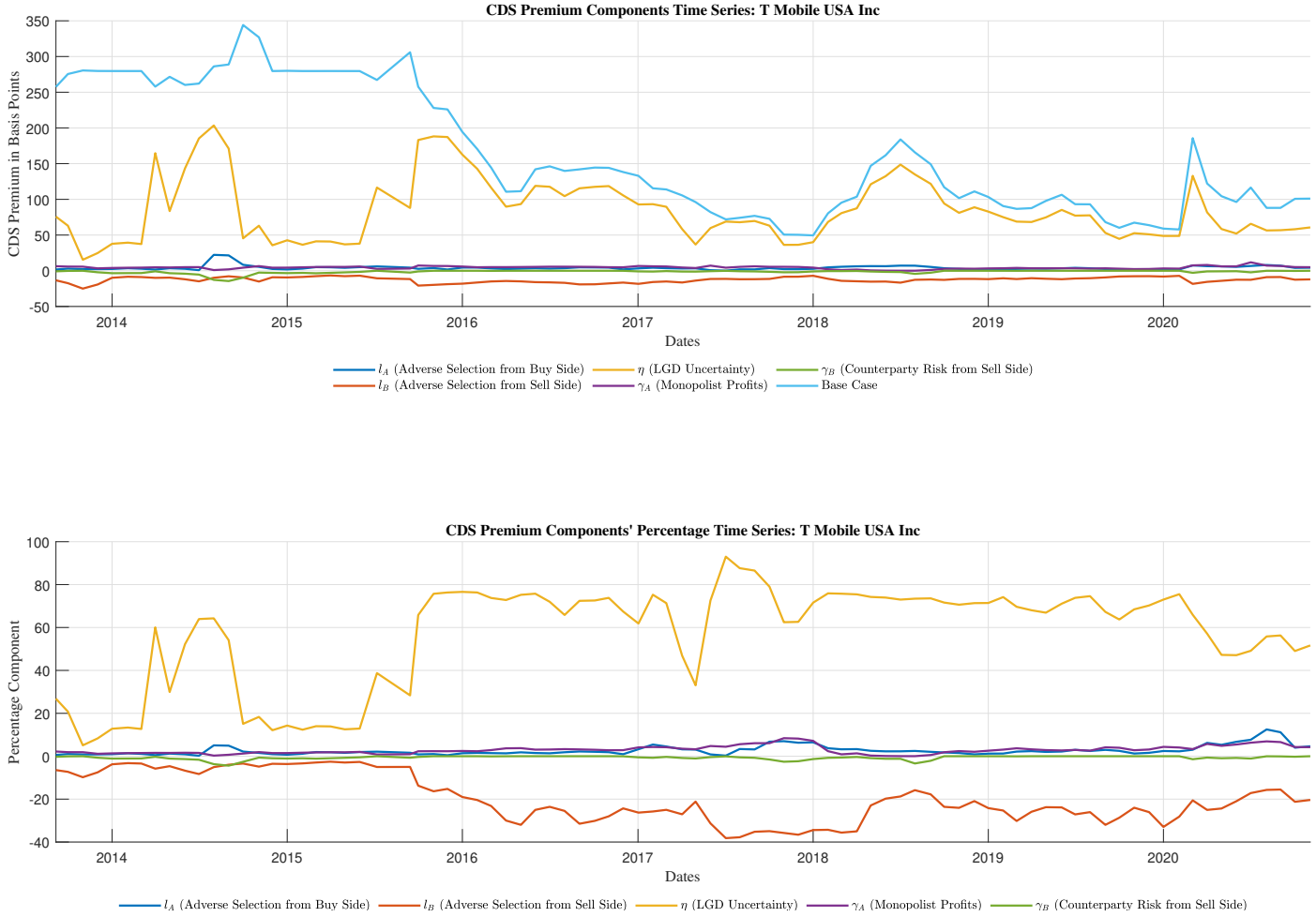

Figure 10: Term structure distributions of the bid-ask spread components

This figure presents the full sample term structure distributions of the different components in the bid-ask spreads. Panel (a) presents the distributions in absolute terms and Panel (b) presents the distributions in percentage terms relative to the full bid-ask spread. The different components are adverse selection from buy side, adverse selection from sell side, recovery-related liquidity, monopolist profits, and counterparty risk. The maturities range from six-month to 10-year. The unit of the y-axis in the upper (lower) panel is basis-point (percent). The green line is the median, the dark gray area is the 25 to 75 percentiles, and the light gray area is the 10 to 90 percentiles.

(a) Actual spreads

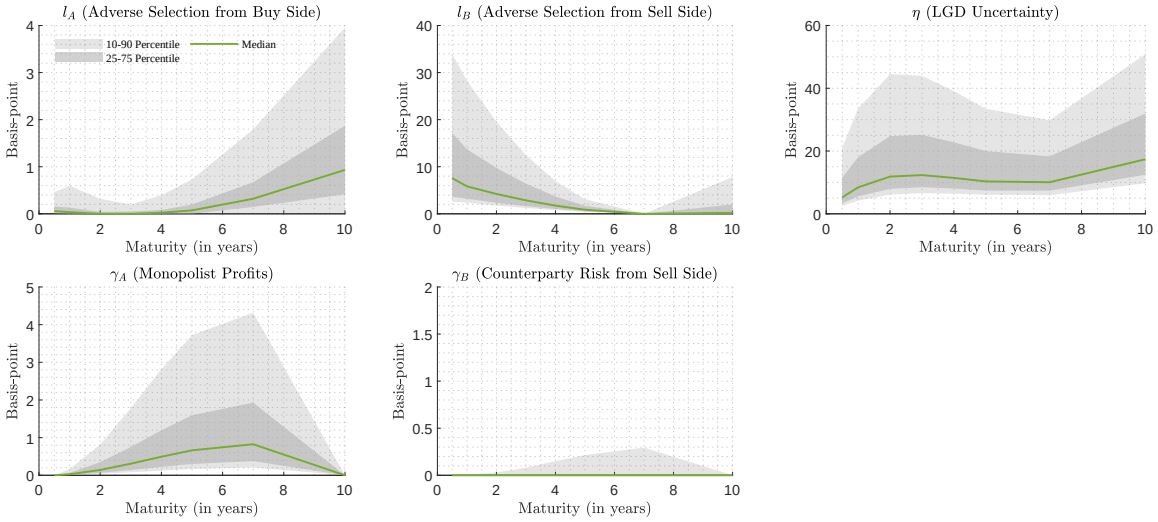

(b) Percentage spreads

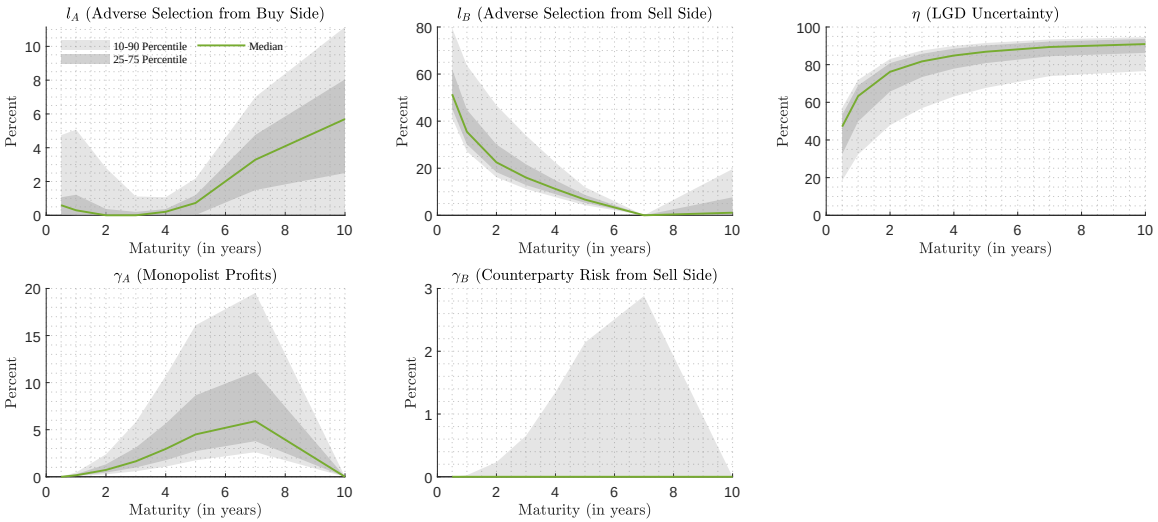

Figure 11: Cross-sectional distributions the bid-ask spread components over time (five-year maturity)

This figure presents the full sample cross-sectional distributions of the different components in the bid-ask spreads of the five-year CDS from November 2011 to August 2017. Panel (a) presents the distributions in absolute terms and Panel (b) presents the distributions in percentage terms relative to the full bid-ask spread. The different components are adverse selection from buy side, adverse selection from sell side, recovery-related liquidity, monopolist profits, and counterparty risk. The unit of the y-axis in the upper (lower) panel is basis-point (percent). The green line is the median, the dark gray area is the 25 to 75 percentiles, and the light gray area is the 10 to 90 percentiles.

(a) Actual spreads

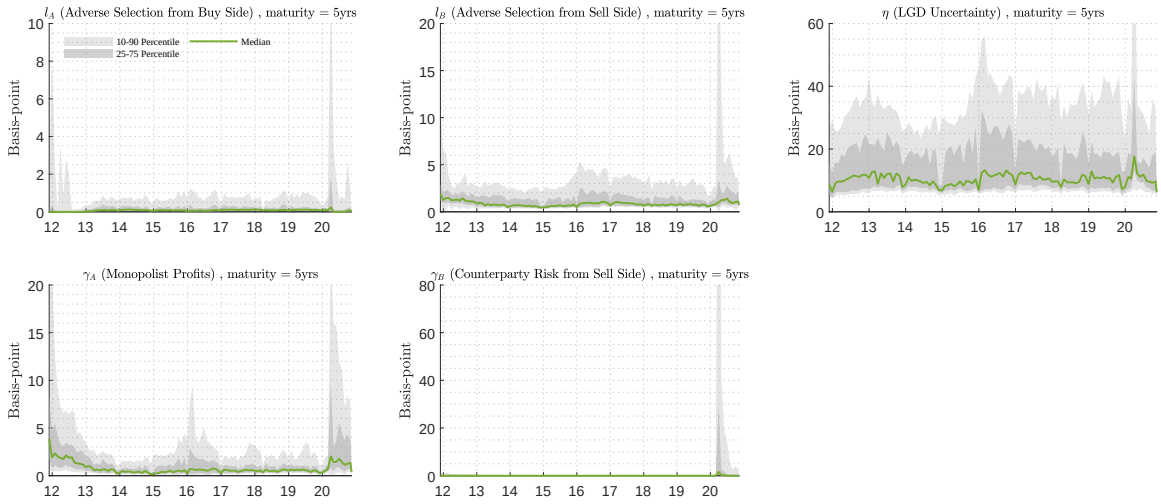

(b) Percentage spreads

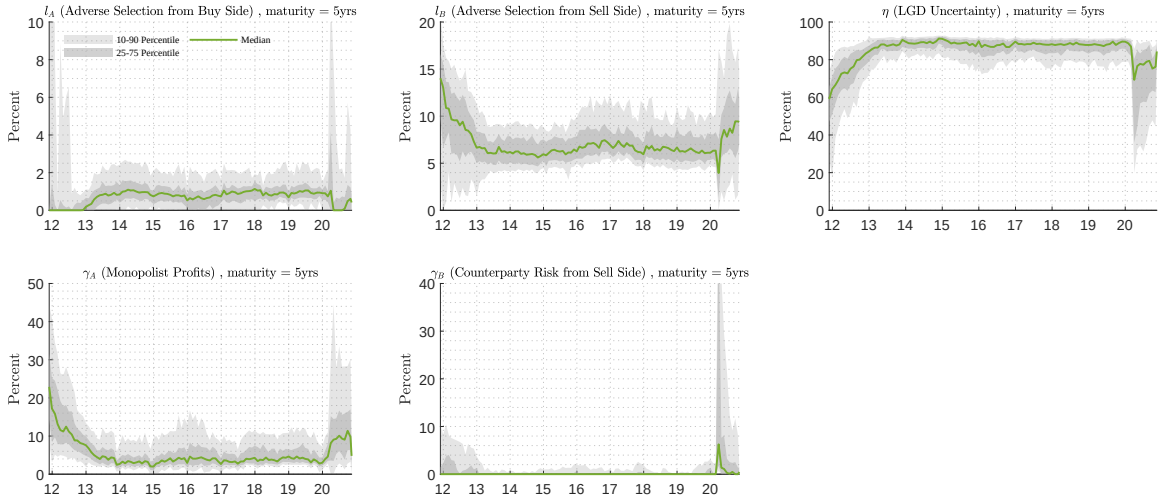

Figure 12: Distributions of the inventory costs

This figure plots the term structure (Panel a) and time series (Panel b) distributions of the inventory costs in terms of bid-ask spread difference due to $\alpha l_A^0 = l_B^0 - l_B$ (left panels) and $\beta l_B^0 = l_A^0 - l_A$ (right panels). The maturities range from one-year to 10-year. The time series in Panel b represents the average value across the maturities. The unit of the y-axis in both panels is basis-point. The green line is the median, the dark gray area is the 25 to 75 percentiles, and the light gray area is the 10 to 90 percentiles.

(a) Term structure

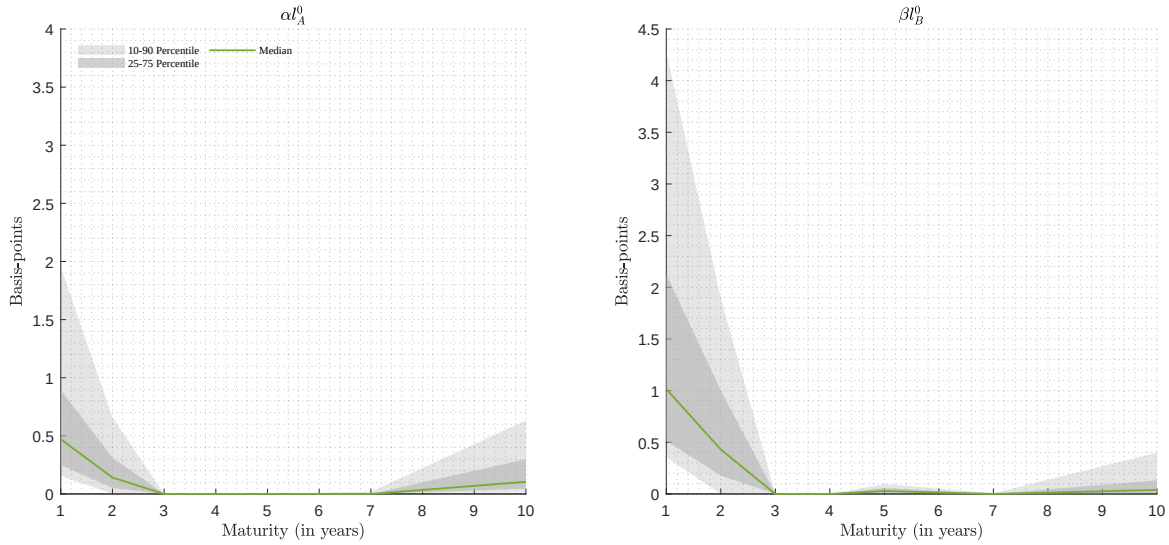

(b) Time series

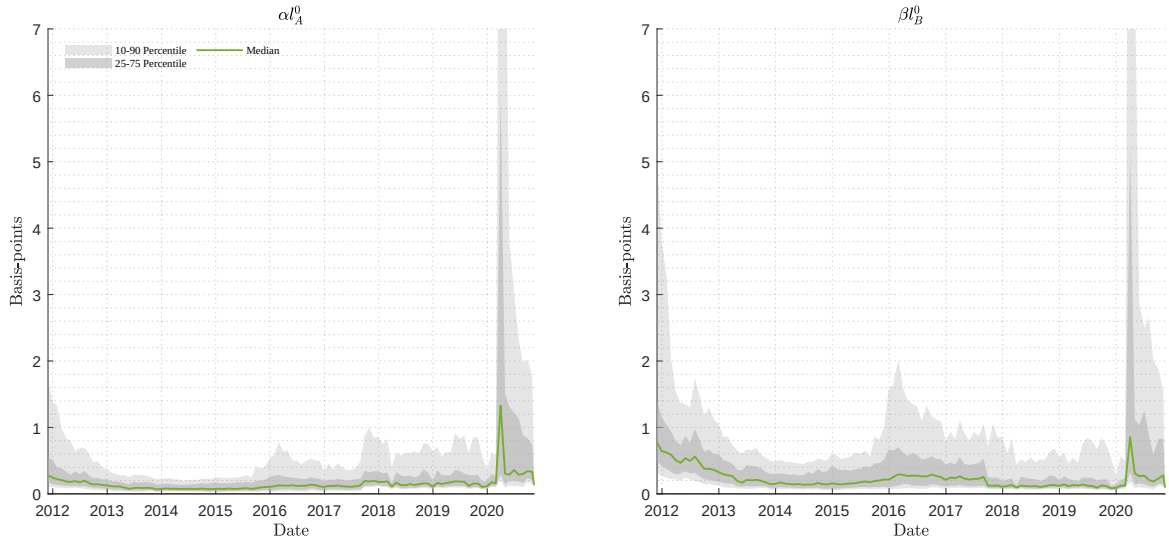

Table 1: Summary descriptives of the data

This table presents the summary statistics of CDS mid quotes, bid-ask spreads, and relative spreads at one-, five- and 10-year maturities. The relative spreads is the ratio of the bid-ask spreads to the CDS mid quotes. In the table, 10 percentile, median, mean, 90 percentile and standard deviation are reported. For the CDS mid quotes and the bid-ask spreads, the figures are in basis-points, while for the relative spreads, the figures are in percent.

	Maturity	10 prcntl	Median	Mean	90 prcntl	STD
CDS mid quote	1	5.04	14.53	92.30	108.15	571.98
	5	26.61	79.09	212.40	458.79	646.37
	10	53.29	126.04	255.27	548.87	541.18
Bid-ask spreads	1	7.32	12.91	31.84	44.11	134.06
	5	5.00	7.75	20.15	24.29	268.91
	10	9.99	17.00	35.98	46.09	229.04
Relative spreads	1	33.78	89.85	101.16	181.05	62.21
	5	4.74	9.03	11.43	20.90	7.97
	10	7.43	13.13	15.18	25.05	8.87

Table 2: Regressing the components to the market-wide liquidity

This table presents the parameter estimates for the NOISE regressions, whose RHS and LHS variables are in the first column and the first row, respectively. The subscripts i, t, and $t-1$ are dropped to save space. The lagged variables are at $t-1$ and others are at t. Weekly data are used in the regressions. The LHS variables are from t and the RHS ones are from $t-1$. The firm fixed effect are controlled in the regressions. The asterisks on top of some estimates denote the level of significance: * is at 10%, ** is at 5%, and *** is at 1% or higher. The reported significance is robust to heteroscedasticity and autocorrelation.

RHS \ LHS	$\Delta BAS(5yr)$	$\Delta\overline{l_A}$	$\Delta\overline{l_B}$	$\Delta\eta$	$\Delta\overline{\gamma_A}$	$\Delta\overline{\gamma_B}$	$\Delta\lambda$
Δ NOISE	0.670***	-0.020	0.042	11.412**	-0.009	-0.003	0.569
lagged Δ NOISE	0.706***	-0.027**	0.039	10.646**	-0.001	0.000	1.526**
lagged LHS	0.057***	-0.214***	-0.205***	-0.185***	-0.269***	-0.196***	-0.128***

Table 3: Panel regression results

The panels in this table present the parameter estimates for the predictive panel regressions, whose RHS and LHS variables are in the first column and the first row, respectively. The subscripts i, t, and $t-1$ are dropped to save space. Daily data are used in the regressions. The LHS variables are from t and the RHS ones are from $t-1$. The firm fixed effect and time fixed effect are controlled in the regressions. Panel (a) is the full sample results, Panel (b) is the top rating group's results, Panel (c) is the mid rating group's results, and Panel (d) is the low rating group's results. The percentage each group accounts for in the full sample is shown in the respective subtitles. The asterisks on top of some estimates denote the level of significance: * is at 10%, ** is at 5%, and *** is at 1% or higher. The reported significance is robust to heteroscedasticity and autocorrelation. † For LHS $= \Delta bid(5yr)$, the second RHS is $\Delta l_B(5yr)$ instead of $\Delta\overline{l_B}$.

(a) Full sample

RHS \ LHS	$\Delta mid(5yr)$	$\Delta ask(5yr)$	$\Delta bid(5yr)$
$\Delta\overline{l_A}$	0.213**	0.222*	0.208**
$\Delta\overline{l_B}^{\dagger}$	-0.085*	-0.103*	-0.589***
$\Delta\eta$	0.003***	0.003***	0.002***
$\Delta\overline{\gamma_A}$	-0.004	0.008	-0.053
$\Delta\overline{\gamma_B}$	0.246	0.280	0.056
$\Delta\lambda$	0.024***	0.027***	0.022***
$\Delta BAS(5yr)$	0.100	-0.021	0.229***
R^2	0.14	0.13	0.14

(b) AAA, AA, and A (35% of full sample)

RHS \ LHS	$\Delta mid(5yr)$	$\Delta ask(5yr)$	$\Delta bid(5yr)$
$\Delta\overline{l_A}$	-0.191	-0.201	-0.180
$\Delta\overline{l_B}$	-0.279***	-0.289***	-0.269***
$\Delta\eta$	0.002***	0.002***	0.002***
$\Delta\overline{\gamma_A}$	0.772***	0.684***	0.860***
$\Delta\overline{\gamma_B}$	0.492	0.573	0.411
$\Delta\lambda$	0.018***	0.020***	0.016***
$\Delta BAS(5yr)$	0.161***	0.062	0.261***
R^2	0.19	0.19	0.20

(c) BBB and BB (43% of full sample)

RHS \ LHS	$\Delta mid(5yr)$	$\Delta ask(5yr)$	$\Delta bid(5yr)$
$\Delta\overline{l_A}$	0.109	0.136	0.085
$\Delta\overline{l_B}$	-0.222***	-0.255***	-0.192***
$\Delta\eta$	0.002***	0.002***	0.002***
$\Delta\overline{\gamma_A}$	-0.171	-0.141	-0.215
$\Delta\overline{\gamma_B}$	0.406	0.343	0.485
$\Delta\lambda$	0.022***	0.025***	0.019***
$\Delta BAS(5yr)$	0.281***	0.177**	0.386***
R^2	0.21	0.21	0.21

(d) B, CCC, and D (22% of full sample)

RHS \ LHS	$\Delta mid(5yr)$	$\Delta ask(5yr)$	$\Delta bid(5yr)$
$\Delta\overline{l_A}$	0.237*	0.242*	0.232**
$\Delta\overline{l_B}$	-0.077	-0.097	-0.056
$\Delta\eta$	0.003***	0.003***	0.002***
$\Delta\overline{\gamma_A}$	-0.058	-0.048	-0.068
$\Delta\overline{\gamma_B}$	0.410*	0.429*	0.391*
$\Delta\lambda$	0.030***	0.035***	0.025***
$\Delta BAS(5yr)$	0.03	-0.100	0.161***
R^2	0.24	0.24	0.25

Table 4: Double sorting average high-minus-low portfolio returns

This table presents the double sorting high-minus-low (HmL) portfolio returns. The first level sorting variable is the monthly average mid quotes in a formation month: the full sample is sorted into three groups (the low, mid, and high in the third to fifth columns in this table), the full sample is kept as another group (the second column in this table). The second level sorting variables are shown in the first column in this table. Other than $\overline{BAS}$ which is the average observed Bid-Ask quote spreads across maturities, all second level sorting variables are the average percentage components relative BAS across maturities. Within each first level group, the firms are further sorted into three subgroups by the monthly average of one second level sorting variable within a formation month. The average HmL is the time series mean of the difference between simple averages of log CDS returns from the high and low portfolios in testing months (one month after formation months). The asterisks on top of some returns denote the level of t-test significance: * is at 10%, ** is at 5%, and *** is at 1% or higher. The figures are monthly log CDS returns in percentage.

Variables	Full sample	Low	Mid	High
$\overline{BAS}$	-0.52	-0.15	-0.68	-0.05
$\overline{l_A}$	0.57*	0.66	0.71	0.41
$\overline{l_B}$	-0.96*	-0.95**	-0.44	-0.64
$\overline{l_A} - \overline{l_B}$	1.16**	0.90**	0.61	0.67
η	0.42	0.37	0.02	0.29
$\overline{\gamma_A}$	-1.22***	-1.01**	-0.58	-0.94
$\overline{\gamma_B}$	0.00	0.21	-0.42	-0.70

Table 5: Regression results of the inventory costs

This table presents α and β from the following regressions:

$$\Delta l_{B,t,i}(\text{n-year}) = c^1_{t,i} - \alpha(\text{n-year})\Delta l_{A,t,i}(\text{n-year}) + \varepsilon^1_{t,i},$$
$$\Delta l_{A,t,i}(\text{n-year}) = c^2_{t,i} - \beta(\text{n-year})\Delta l_{B,t,i}(\text{n-year}) + \varepsilon^2_{t,i}.$$

where $n = 1, 2, 3, 5, 7$ and 10. Daily data are used in the regressions. The firm fixed effect and time fixed effect are controlled in the regressions. The asterisks on top of some estimates denote the level of significance: * is at 10%, ** is at 5%, and *** is at 1% or higher. The reported significance is robust to heteroscedasticity and autocorrelation.

	1-year	2-year	3-year	5-year	7-year	10-year
α	0.516***	0.189	-0.066	0.015*	0.055***	0.378***
β	0.132***	0.067	-0.060	0.196	0.325***	0.073***

Appendices

A Proof of Proposition 1

Define $h(x,\eta;\tau) \equiv \frac{g(x+\eta,\tau)}{g(x,\tau)}$. Since all functions defined here are continuous and differentiable up to the second order, this condition is satisfied by default wherenever needed without stating. We first show $\frac{\partial g(x,\tau)}{\partial x} < 0$ and $\frac{\partial h(x,\eta;\tau)}{\partial x} > 0$, for $x > 0$, $\eta \geq 0$, and $\tau > 0$. To this end, we have

$$\frac{\partial g(x,\tau)}{\partial x} = -\frac{\frac{1}{x} - \left(\frac{1}{x}+\tau\right)e^{-x\tau}}{x} < 0, \tag{A1}$$

$$\frac{\partial^2 g(x,\tau)}{\partial x^2} = \frac{\frac{1}{x^2} - \left(\frac{1}{x}+\tau\right)^2 e^{-x\tau}}{x} > 0, \tag{A2}$$

and

$$\frac{\partial h(x,\eta;\tau)}{\partial x} = \frac{\frac{\partial g(x+\eta,\tau)}{\partial x} g(x,\tau) - \frac{\partial g(x,\tau)}{\partial x} g(x+\eta,\tau)}{g(x,\tau)^2},$$

given (A1) and (A2), apparently $\frac{\partial h(x,\eta;\tau)}{\partial x} > 0$.

A.1 $\frac{\partial s_{\Delta t}}{\partial \lambda} > w$, $\frac{\partial s_{A,\Delta t}}{\partial \lambda_A} > w$, and $\frac{\partial s_{B,\Delta t}}{\partial \lambda_B} > 0$:

We now show $\frac{\partial s_{\Delta t}}{\partial \lambda} > w$:

$$\frac{\partial s_{\Delta t}(\lambda,\eta)}{\partial \lambda} = \frac{\partial\left\{\lambda\left[1-h(\lambda,\eta;\Delta t)(1-w)\right]\right\}}{\partial \lambda} = 1 - \left\{h(\lambda,\eta;\Delta t) + \lambda\frac{\partial h(\lambda,\eta;\Delta t)}{\partial \lambda}\right\}(1-w).$$

$$\frac{\partial^2 s_{\Delta t}(\lambda,\eta)}{\partial \lambda \partial \eta} = -(1-w)\left(\frac{\partial h(\lambda,\eta;\Delta t)}{\partial \eta} + \lambda\frac{\partial^2 h(\lambda,\eta;\Delta t)}{\partial \lambda \partial \eta}\right),$$

where $\frac{\partial h(\lambda,\eta;\Delta t)}{\partial \eta} = \frac{\frac{\partial g(\lambda+\eta,\Delta t)}{\partial \eta}}{g(\lambda,\Delta t)} < 0$ and

$$\begin{aligned}
&\frac{\partial^2 h\left(\lambda,\eta;\Delta t\right)}{\partial\lambda\partial\eta} \\
&= \frac{\frac{\partial^2 g(\lambda+\eta,\Delta t)}{\partial\lambda\partial\eta} g\left(\lambda,\Delta t\right) - \frac{\partial g(\lambda,\Delta t)}{\partial\lambda}\frac{\partial g(\lambda+\eta,\Delta t)}{\partial\eta}}{g\left(\lambda,\Delta t\right)^2} \\
&< \frac{\frac{\partial^2 g(\lambda+\eta,\Delta t)}{\partial\lambda\partial\eta} g\left(\lambda+\eta,\Delta t\right) - \left[\frac{\partial g(\lambda+\eta,\Delta t)}{\partial\eta}\right]^2}{g\left(\lambda,\Delta t\right)^2} \\
&= \frac{\left(1-e^{-(\lambda+\eta)\Delta t}\right)\left[\frac{1}{(\lambda+\eta)^2} - \left(\frac{1}{(\lambda+\eta)}+\Delta t\right)^2 e^{-(\lambda+\eta)\Delta t}\right] - \left[\frac{1}{(\lambda+\eta)} - \left(\frac{1}{(\lambda+\eta)}+\Delta t\right)e^{-(\lambda+\eta)\Delta t}\right]^2}{\left(\lambda+\eta\right) g\left(\lambda,\Delta t\right)^2} \\
&= -\frac{\left(\Delta t\right)^2 e^{-(\lambda+\eta)\Delta t}}{\left(\lambda+\eta\right) g\left(\lambda,\Delta t\right)^2} < 0.
\end{aligned}$$

Therefore, $\frac{\partial^2 s_{\Delta t}(\lambda,\eta)}{\partial\lambda\partial\eta} > 0$ and $\frac{\partial s_{\Delta t}(\lambda,\eta)}{\partial\lambda} > \lim_{\eta\to 0}\frac{\partial s_{\Delta t}(\lambda,\eta)}{\partial\lambda} = w$.

For $\frac{\partial s_{A,\Delta t}}{\partial\lambda_A} > w$, we write $s_{A,\Delta t}\left(\lambda_A,\gamma_A,\eta\right) = \frac{s_{\Delta t}(\lambda_A,\eta)}{h(\lambda_A,\gamma_A;\Delta t)}$ and $\frac{\partial s_{A,\Delta t}}{\partial\lambda_A} = \frac{\Theta(\lambda_A,\gamma_A,\eta)}{h(\lambda_A,\gamma_A;\Delta t)^2}$ where

$$\Theta\left(\lambda_A,\gamma_A,\eta\right) = \frac{\partial s_{\Delta t}\left(\lambda_A,\eta\right)}{\partial\lambda_A} h\left(\lambda_A,\gamma_A;\Delta t\right) - s_{\Delta t}\left(\lambda_A,\eta\right)\frac{\partial h\left(\lambda_A,\gamma_A;\Delta t\right)}{\partial\lambda_A}.$$

Taking the partial derivatives of $\Theta\left(\lambda_A,\gamma_A,\eta\right)$ with respect to η, we have

$$\begin{aligned}
\frac{\partial\Theta\left(\lambda_A,\gamma_A,\eta\right)}{\partial\eta} &= \frac{\partial^2 s_{\Delta t}\left(\lambda_A,\eta\right)}{\partial\lambda_A\partial\eta} h\left(\lambda_A,\gamma_A;\Delta t\right) - \frac{\partial s_{\Delta t}\left(\lambda_A,\eta\right)}{\partial\eta}\frac{\partial h\left(\lambda_A,\gamma_A;\Delta t\right)}{\partial\lambda_A} \\
&= \left(1-w\right)\frac{\partial h\left(\lambda_A,\eta;\Delta t\right)}{\partial\eta}\left[\lambda\frac{\partial h\left(\lambda_A,\gamma_A;\Delta t\right)}{\partial\lambda_A} - h\left(\lambda_A,\gamma_A;\Delta t\right)\right] \\
&\quad - \left(1-w\right)\lambda h\left(\lambda_A,\gamma_A;\Delta t\right)\frac{\partial h^2\left(\lambda_A,\eta;\Delta t\right)}{\partial\lambda_A\partial\eta} \\
&> \left(1-w\right)\frac{\partial h\left(\lambda_A,\eta;\Delta t\right)}{\partial\eta}\left[\lambda\frac{\partial h\left(\lambda_A,\gamma_A;\Delta t\right)}{\partial\lambda_A} - h\left(\lambda_A,\gamma_A;\Delta t\right)\right]
\end{aligned}$$

where the last inequality is by $\frac{\partial h^2(\lambda_A,\eta;\Delta t)}{\partial\lambda_A\partial\eta} < 0$. We also have

$$\begin{aligned}
\lambda\frac{\partial h\left(\lambda_A,\gamma_A;\Delta t\right)}{\partial\lambda_A} - h\left(\lambda_A,\gamma_A;\Delta t\right) &= \frac{\lambda_A\frac{\partial g(\lambda_A+\eta,\Delta t)}{\partial\lambda_A}}{g\left(\lambda_A,\Delta t\right)} - h\left(\lambda_A,\gamma_A;\Delta t\right)\left[1+\frac{\lambda_A\frac{\partial g(\lambda_A,\Delta t)}{\partial\lambda_A}}{g\left(\lambda_A,\Delta t\right)}\right] \\
&= \frac{\lambda_A\frac{\partial g(\lambda_A+\eta,\Delta t)}{\partial\lambda_A}}{g\left(\lambda_A,\Delta t\right)} - h\left(\lambda_A,\gamma_A;\Delta t\right)\left[1-\frac{1-\left(1+\lambda\Delta t\right)e^{-\lambda_A\Delta t}}{1-e^{-\lambda_A\Delta t}}\right] \\
&= \frac{\lambda_A\frac{\partial g(\lambda_A+\eta,\Delta t)}{\partial\lambda_A}}{g\left(\lambda_A,\Delta t\right)} - h\left(\lambda_A,\gamma_A;\Delta t\right)\frac{\lambda_A\Delta t}{e^{\lambda_A\Delta t}-1} < 0,
\end{aligned}$$

where the last inequality is by $\frac{\partial g(\lambda_A+\eta,\Delta t)}{\partial\lambda_A} < 0$. Therefore, together with $\frac{\partial h(\lambda_A,\eta;\Delta t)}{\partial\eta} < 0$, we have shown $\frac{\partial\Theta(\lambda_A,\gamma_A,\eta)}{\partial\eta} > 0$ and

$$\frac{\partial s_{A,\Delta t}\left(\lambda_A,\gamma_A,\eta\right)}{\partial\lambda_A} > \frac{\lim_{\eta\to 0}\Theta\left(\lambda_A,\gamma_A,\eta\right)}{h\left(\lambda_A,\gamma_A;\Delta t\right)^2} = \frac{w}{h\left(\lambda_A,\gamma_A;\Delta t\right)} > w.$$

For $\frac{\partial s_{B,\Delta t}}{\partial\lambda_B} > 0$, we write $s_{B,\Delta t}\left(\lambda_B,\gamma_B,\eta\right) = \frac{\lambda_B h(\lambda_B,\gamma_A;\Delta t)}{\lambda_B+\gamma_B} s_{\Delta t}\left(\lambda_B+\gamma_B,\eta\right)$ and

$$\frac{\partial s_{B,\Delta t}}{\partial\lambda_B} = \frac{\gamma_B}{\left(\lambda_B+\gamma_B\right)^2}\Psi\left(\lambda_B,\gamma_B,\eta\right) + \frac{\lambda_B}{\lambda_B+\gamma_B}\frac{\partial\Psi\left(\lambda_B,\gamma_B,\eta\right)}{\partial\lambda_B},$$

where $\Psi\left(\lambda_B,\gamma_B,\eta\right) = h\left(\lambda_B,\gamma_A;\Delta t\right)s_{\Delta t}\left(\lambda_B+\gamma_B,\eta\right)$. Since $\frac{\partial h(\lambda_B,\gamma_A;\Delta t)}{\partial\lambda_B} > 0$ and $\frac{\partial s_{\Delta t}(\lambda_B+\gamma_B,\eta)}{\partial\lambda_B} > 0$, we have $\frac{\partial\Psi(\lambda_B,\gamma_B,\eta)}{\partial\lambda_B} > 0$. This proves $\frac{\partial s_{B,\Delta t}}{\partial\lambda_B} > 0$.

A.2 $BA_{\Delta t} = s_{A,\Delta t} - s_{B,\Delta t}$ is positive

Now to see $s_{A,\Delta t} > s_{B,\Delta t}$, we have

$$\begin{aligned}
s_{A,\Delta t} &= \lambda_A \frac{g(\lambda_A, \Delta t)}{g(\lambda_A + \gamma_A, \Delta t)} \left[1 - \frac{g(\lambda_A + \eta, \Delta t)}{g(\lambda_A, \Delta t)} (1 - w)\right] \\
&> \lambda_A \left[1 - \frac{g(\lambda_A + \eta, \Delta t)}{g(\lambda_A, \Delta t)} (1 - w)\right] \\
&> \lambda_B \left[1 - \frac{g(\lambda_B + \eta, \Delta t)}{g(\lambda_B, \Delta t)} (1 - w)\right] \\
&> \lambda_B \left[1 - \frac{g(\lambda_B + \gamma_B + \eta, \Delta t)}{g(\lambda_B + \gamma_B, \Delta t)} (1 - w)\right] \\
&> \lambda_B \frac{g(\lambda_B + \gamma_B, \Delta t)}{g(\lambda_B, \Delta t)} \left[1 - \frac{g(\lambda_B + \gamma_B + \eta, \Delta t)}{g(\lambda_B + \gamma_B, \Delta t)} (1 - w)\right] \\
&= s_{B,\Delta t}.
\end{aligned}$$

The first inequality is by $\frac{g(\lambda_A, \Delta t)}{g(\lambda_A + \gamma_A, \Delta t)} > 1$, the second is by $\frac{\partial s_{\Delta t}}{\partial \lambda} > 0$ and $\lambda_A > \lambda_B$, the third is by $\frac{\partial \left[\frac{g(x+\eta,\tau)}{g(x,\tau)}\right]}{\partial x} > 0$, and the last is by $\frac{g(\lambda_B + \gamma_B, \Delta t)}{g(\lambda_B, \Delta t)} < 1$.

A.3 $\frac{\partial BA_{\Delta t}}{\partial \gamma_A} > 0$, $\frac{\partial BA_{\Delta t}}{\partial \gamma_B} > 0$, $\frac{\partial BA_{\Delta t}}{\partial l_A} > 0$, and $\frac{\partial BA_{\Delta t}}{\partial l_B} > 0$

Given $\frac{\partial g(x,\tau)}{\partial x} < 0$, we have $\frac{\partial s_{A,\Delta t}}{\partial \gamma_A} > 0$ and $\frac{\partial BA_{\Delta t}}{\partial \gamma_A} > 0$; given $\frac{\partial g(x,\tau)}{\partial x} < 0$ and $\frac{\partial \left[\frac{g(x+\eta,\tau)}{g(x,\tau)}\right]}{\partial x} > 0$, we have $\frac{\partial s_{B,\Delta t}}{\partial \gamma_B} < 0$, therefore $\frac{\partial BA_{\Delta t}}{\partial \gamma_B} > 0$; given $\frac{\partial s_{A,\Delta t}}{\partial \lambda} > 0$, we have $\frac{\partial BA_{\Delta t}}{\partial l_A} > 0$; given $\frac{\partial s_{B,\Delta t}}{\partial l_B} < 0$, we have $\frac{\partial BA_{\Delta t}}{\partial l_B} > 0$.

A.4 $\frac{\partial BA_{\Delta t}}{\partial w} > 0$ if $\gamma_A > \eta$, and $\frac{\partial BA_{\Delta t}}{\partial \eta} > 0$ if $l_A + l_B > \gamma_B$

By definition, we have

$$\frac{\partial s_{A,\Delta t}}{\partial w} = \lambda_A \frac{g(\lambda_A + \eta, \Delta t)}{g(\lambda_A + \gamma_A, \Delta t)} w.$$

When $\gamma_A > \eta$,

$$\frac{\partial s_{A,\Delta t}}{\partial w} > \lambda_A w > \lambda_B w > \lambda_B \frac{g\left(\lambda_B + \gamma_B + \eta, \Delta t\right)}{g\left(\lambda_B, \Delta t\right)} w = \frac{\partial s_{B,\Delta t}}{\partial w},$$

therefore $\frac{\partial BA_{\Delta t}}{\partial w} > 0$.

Similarly, we have

$$\begin{aligned}
\frac{\partial s_{A,\Delta t}}{\partial \eta} &= -\frac{\lambda_A}{h\left(\lambda_A, \gamma_A; \Delta t\right)} \frac{\partial h\left(\lambda_A, \eta; \Delta t\right)}{\partial \eta} \left(1 - w\right), \\
\frac{\partial s_{B,\Delta t}}{\partial \eta} &= -\lambda_B h\left(\lambda_B, \gamma_B; \Delta t\right) \frac{\partial h\left(\lambda_B + \gamma_B, \eta; \Delta t\right)}{\partial \eta} \left(1 - w\right), \\
\frac{\partial BA_{\Delta t}}{\partial \eta} &= \left(1 - w\right) \left[\lambda_B h\left(\lambda_B, \gamma_B; \Delta t\right) \frac{\partial h\left(\lambda_B + \gamma_B, \eta; \Delta t\right)}{\partial \eta} - \frac{\lambda_A}{h\left(\lambda_A, \gamma_A; \Delta t\right)} \frac{\partial h\left(\lambda_A, \eta; \Delta t\right)}{\partial \eta}\right] \\
&> \left(1 - w\right) \lambda_B h\left(\lambda_B, \gamma_B; \Delta t\right) \left[\frac{\partial h\left(\lambda_B + \gamma_B, \eta; \Delta t\right)}{\partial \eta} - \frac{\partial h\left(\lambda_A, \eta; \Delta t\right)}{\partial \eta}\right].
\end{aligned}$$

When $l_A + l_B > \gamma_B \Rightarrow \lambda_A > \lambda_B + \gamma_B$, together with $\frac{\partial h(\lambda, \eta; \Delta t)}{\partial \lambda} < 0$, we have $\frac{\partial BA_{\Delta t}}{\partial \eta} > 0$.

Proof of Proposition 1 finishes.

B Specification analysis

In our model, we assume the different factors are constant. Empirically, We recalibrate the model on a daily basis which essentially allows for time varying factors, but in an inconsistent manner. This is a common practice in the industry. For example, the implied volatility computed from observed option prices on a time varying basis is a constant parameter in the Black-Scholes option pricing model. In this appendix, we show that the recalibration of our model can pick up the time variation in factors reasonably well from bid-ask spreads simulated based on a more dynamic and consistent model.

To illustrate the point while remaining tractable, we only allow the default intensity λ to be a stochastic process, λ_t, and keep other factors constant. Specifically, we assume λ_t follows a CIR

process (Longstaff, Mithal, and Neis, 2005):

$$d\lambda_t = (\alpha - \beta\lambda_t)\, dt + \sigma\sqrt{\lambda_t} dw_t, \tag{A3}$$

where w_t is a Wiener process under the risk neutral measure. Consider a maturity of Δt at time t, for the ask quote, the premium leg $Q_{A,t}$ and the protection leg $P_{A,t}$ are given by

$$\begin{aligned}
Q_{A,t} &= s_{A,t} \int_t^{t+\Delta t} \mathbb{E}_t \left[\exp\left(- \int_t^\tau \lambda_s + l_A + \gamma_A ds \right) \right] d\tau \\
&= s_{A,t} \int_t^{t+\Delta t} e^{-(l_A+\gamma_A)(\tau - t)} \mathbb{E}\left[\exp\left(- \int_t^\tau \lambda_s ds \right) \right] d\tau, \\
P_{A,t} &= \int_t^{t+\Delta t} \left[1 - (1-w) e^{-\eta(\tau - t)} \right] \mathbb{E}_t \left[(\lambda_\tau + l_A) \exp\left(- \int_t^\tau \lambda_s + l_A ds \right) \right] d\tau \\
&= \int_t^{t+\Delta t} K(w, l_A, \eta; \tau - t) \left\{ \mathbb{E}_t \left[\lambda_\tau \exp\left(- \int_t^\tau \lambda_s \right) ds \right] + l_A \mathbb{E}_t \left[\exp\left(- \int_t^\tau \lambda_s ds \right) \right] \right\} d\tau,
\end{aligned}$$

where $\mathbb{E}_t(.)$ is the conditional expectation under the risk neutral measure at time t, and $K(a, b, c; \tau)$ is defined as:

$$K(a, b, c; \tau) = \exp(-b\tau) - (1-a)\exp(-b\tau - c\tau).$$

The ask quote for CDS premium equalizes $Q_{A,t}$ and $P_{A,t}$, therefore,

$$s_{A,t} = \frac{\int_t^{t+\Delta t} K(w, l_A, \eta; \tau - t) \left\{ \mathbb{E}_t \left[\lambda_\tau \exp\left(- \int_t^\tau \lambda_s ds \right) \right] + l_A \mathbb{E}_t \left[\exp\left(- \int_t^\tau \lambda_s ds \right) \right] \right\} d\tau}{\int_t^{t+\Delta t} e^{-(l_A+\gamma_A)(\tau - t)} \mathbb{E}\left[\exp\left(- \int_t^\tau \lambda_s ds \right) \right] d\tau}.$$

Similarly, for the bid quote, we have

$$\begin{aligned}
Q_{B,t} &= s_{B,t} \int_t^{t+\Delta t} e^{l_B(\tau - t)} \mathbb{E}\left[\exp\left(- \int_t^\tau \lambda_s ds \right) \right] d\tau, \\
P_{B,t} &= \int_t^{t+\Delta t} K(w, \gamma_B - l_B, \eta; \tau - t) \left\{ \mathbb{E}_t \left[\lambda_\tau \exp\left(- \int_t^\tau \lambda_s ds \right) \right] - l_B \mathbb{E}_t \left[\exp\left(- \int_t^\tau \lambda_s ds \right) \right] \right\} d\tau.
\end{aligned}$$

The bid quote for CDS premium equalizes $Q_{B,t}$ and $P_{B,t}$, therefore,

$$s_{B,t} = \frac{\int_t^{t+\Delta t} K(w, \gamma_B - l_B, \eta; \tau - t) \left\{ \mathbb{E}_t \left[\lambda_\tau \exp\left(- \int_t^\tau \lambda_s ds \right) \right] - l_B \mathbb{E}_t \left[\exp\left(- \int_t^\tau \lambda_s ds \right) \right] \right\} d\tau}{\int_t^{t+\Delta t} e^{l_B(\tau - t)} \mathbb{E}_t \left[\exp\left(- \int_t^\tau \lambda_s ds \right) \right] d\tau}.$$

By the standard affine techniques (see Duffie, Pan, and Singleton, 2000; Longstaff, Mithal, and Neis, 2005),

$$\begin{aligned} \mathbb{E}_t \left[\exp\left(- \int_t^\tau \lambda_s ds \right) \right] &= A(\tau - t) e^{B(\tau - t)\lambda_t}, \\ \mathbb{E}_t \left[\lambda_\tau \exp\left(- \int_t^\tau \lambda_s ds \right) \right] &= \left[G(\tau - t) + H(\tau - t)\lambda_t \right] e^{B(\tau - t)\lambda_t}, \end{aligned}$$

where A, B, G, and H are functions of α, β, σ and $\tau - t$. Their detailed formulas can be found on page 2221 in Longstaff, Mithal, and Neis (2005).

Although this model permits a consistent modeling for the default intensity λ, it adds five more parameters: α, $\alpha^{\mathbb{P}}$, β, $\beta^{\mathbb{P}}$, and σ, where $\alpha^{\mathbb{P}}$ and $\beta^{\mathbb{P}}$ are the physical ($\mathbb{P}$) measure counterparts of α and β. Therefore, the daily stand alone calibration enjoyed by the constant factor model is no longer feasible. A more sophisticated estimation procedure, for example, Kalman filter and maximum likelihood estimation, must be employed. Comparing with the constant factor model, the appealing practicality is missing in this more sophisticated model. We use simulation to check how much rigor is lost from choosing the constant factor model over this more sophisticated model.

Following the same practice in Section 2.4, we allow three free parameters in the term structure function for $l_A(\Delta t)$, $l_B(\Delta t)$, $\gamma_A(\Delta t)$ and $\gamma_B(\Delta t)$ to pin down three values at six-month, five-year, and 10-year then interpolate the term structure curve using spline function to fill the values on any points in between six months and 10 years. We simulate 200 λ_t based on $\alpha^{\mathbb{P}} = 0.15$, $\beta^{\mathbb{P}} = 1.5$, and $\sigma = 0.2$. For pricing the bid and ask CDS premiums, we use the following parameter setting: $\alpha = 0.05$, $\beta = 0.5$, $\eta = 0.06$, $l_A(0.5) = 0.3\lambda_t$, $l_A(5) = 0.2\lambda_t$, $l_A(10) = 0.2\lambda_t$, $l_B(0.5) = 0.4\lambda_t$, $l_B(5) = 0.2\lambda_t$, $l_B(10) = 0.2\lambda_t$, $\gamma_A(0.5) = 0.008$, $\gamma_A(5) = 0.017$,

Figure A1: Simulation results

Panels l_A, l_B, η, γ_A, and γ_B compare five to 95 percentiles and medians of these components' percentage in the bid-ask spreads (over different maturities) from the calibrated constant factor model with their true (simulated) counterparts. The last panel plots the time series of the 200 simulated λ_t against their estimated value from calibrating the constant factor model to the simulated bid and ask CDS premium quotes. The values for parameters used in the simulation are as follows: $\alpha^{\mathbb{P}} = 0.15$, $\beta^{\mathbb{P}} = 1.5$, $\sigma = 0.2$, $\alpha = 0.05$, $\beta = 0.5$, $\eta = 0.06$, $l_A(0.5) = 0.3\lambda_t$, $l_A(5) = 0.2\lambda_t$, $l_A(10) = 0.2\lambda_t$, $l_B(0.5) = 0.4\lambda_t$, $l_B(5) = 0.2\lambda_t$, $l_B(10) = 0.2\lambda_t$, $\gamma_A(0.5) = 0.008$, $\gamma_A(5) = 0.017$, $\gamma_A(10) = 0.013$, $\gamma_B(0.5) = 0.009$, $\gamma_B(5) = 0.016$, and $\gamma_B(10) = 0.014$.

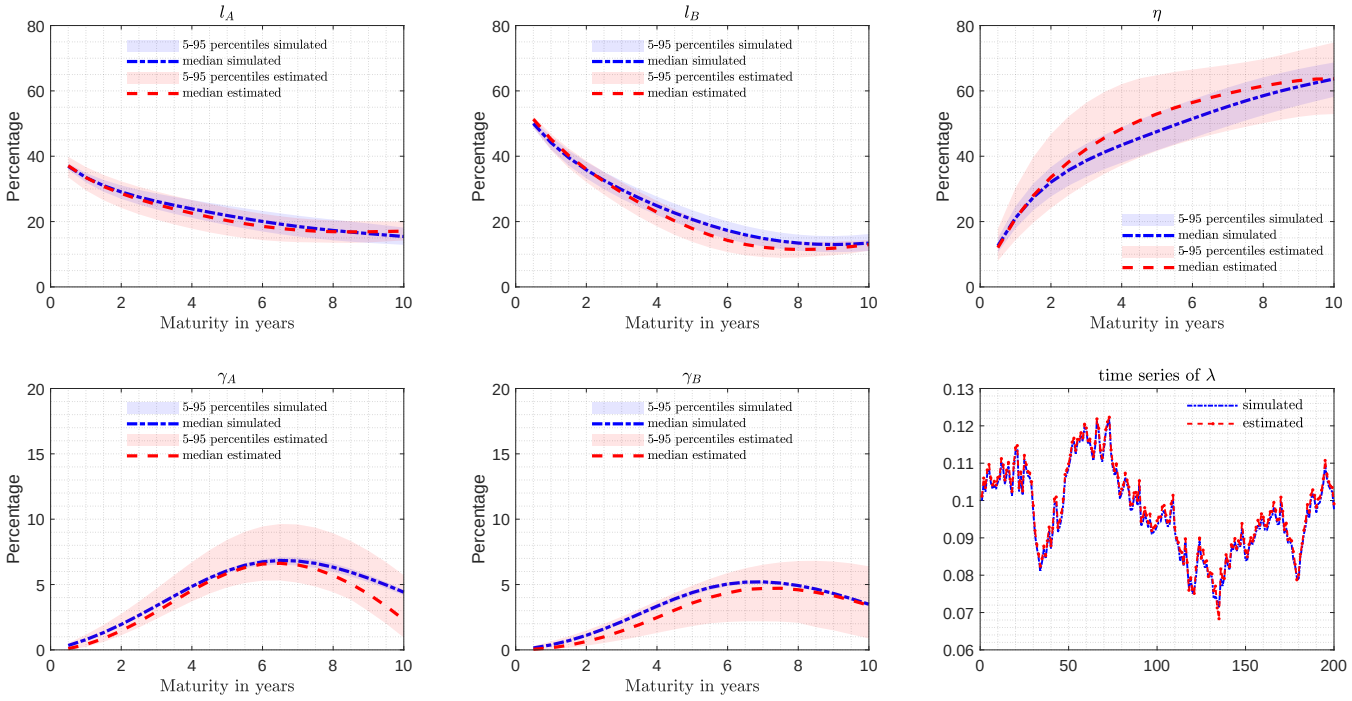

$\gamma_A(10) = 0.013$, $\gamma_B(0.5) = 0.009$, $\gamma_B(5) = 0.016$, and $\gamma_B(10) = 0.014$. We calibrate our model to these simulated bid and ask CDS premium quotes and compare the percentage of different components from the calibrated model with their simulated counterparts. From the comparisons shown in Figure A1, we can clearly see that overall the constant factor model captures the components' percentage in the bid-ask spreads really well. The true values are all within the five percent confidence intervals. Moreover, the key factor λ is assumed to be constant in the constant factor model. By frequent recalibrating, the constant factor model can still capture the time variation generated by the more consistent and dynamic model. This

observation is shown in the last panel of Figure A1 where the estimated λ's are plotted against their true values (the simulated values) and the estimated λ consistently tracks the true value. Therefore, the results from this simulation exercise show that the gain in practicality of the constant factor model outweighs the loss in rigor.